CHALMERS

A computational model of a ground vehicle with engine mounted on rigid chassis

A tool for vibration dynamic analysis and design parameter optimization implemented in MSC Adams View

International Master's Programme Solid and Fluid Mechanics

FELIX GÖBEL

Department of Applied Mechanics
Division of Dynamics
CHALMERS UNIVERSITY OF TECHNOLOGY
Göteborg, Sweden 2009
Master's Thesis 2009:01

MASTER'S THESIS 2009:01

A computational model of a ground vehicle with engine mounted on rigid chassis

A tool for vibration dynamic analysis and design parameter optimization implemented in MSC Adams View

FELIX GÖBEL

Department of Applied Mechanics
Division of Dynamics
CHALMERS UNIVERSITY OF TECHNOLOGY
Göteborg, Sweden 2009

A computational model of a ground vehicle with engine mounted on rigid chassis
A tool for vibration dynamic analysis and design parameter optimization implemented in MSC Adams View

FELIX GÖBEL

© FELIX GÖBEL, VIKTOR BERBYUK, 2009

Master's Thesis 2009:01
ISSN 1652-8557
Department of Applied Mechanics
Division of Dynamics
Chalmers University of Technology
SE-412 96 Göteborg
Sweden
Telephone: + 46 (0)31-772 1000

Chalmers Reproservice
Göteborg, Sweden 2009

A computational model of a ground vehicle with engine mounted on rigid chassis

A tool for vibration dynamic analysis and design parameter optimization implemented in MSC Adams View

FELIX GÖBEL
Department of Applied Mechanics
Division of Dynamics
Chalmers University of Technology

ABSTRACT

Today's automotive manufacturers have to satisfy the growing demand for fuel saving vehicles. To reach that, they try to reduce the weight of the vehicles. But less mass leads to bigger problems with vibrations and that means worse comfort. The two main sources of vibrations in a motorcar are the working process of the engine and the roughness of the road. Especially the vibrations caused by the engine can be reduced by advanced engine mounting systems. A mechanical, mathematical and computational model of a four wheel ground vehicle with focus on the engine mounting system is presented in this paper. The mechanical model consists of rigid bodies for the engine and chassis connected with a three point mounting system, unsprung masses and linear springs and dampers in parallel for the tires and suspension. The mounts are also modelled as linear springs and dampers in parallel but with independent parameters in three directions. All in all it has 13 degrees of freedom. The differential equations describing the model were derived. The computational model implemented in MSC Adams View provides the possibility for vibration dynamic analysis of a vehicle under different dynamic excitations coming from the engine and kinematic excitations coming from the road. Since it is completely parameterised it is easily possible to customize it to any four wheel ground vehicle with three point engine mounting system. In connection with the build in Adams View optimizer tool design parameter optimization is possible. Furthermore some examples to demonstrate the power of the model are shown. The focus is put on the optimization of the damping of the engine mounts. It shows that for different sets of excitations different sets of damping parameters are optimal, in a sense that they result in less vibrations of the chassis which means better comfort. The achievable improvements compared to the conventional mounting system look very promising, even if the number of different combinations of excitations is too small to make significant predictions. The application of this could be an adaptive mounting system, utilizing electro- or magneto-rheological mounts or such with a tunable bypass valve, which is able to switch its damping properties depending on the state of the engine and road to gain better comfort.

Key words:

Engine mounting system, four wheel ground vehicle, adaptive mounting system, conventional mounting system, MSC Adams View, mechanical model, mathematical model, computational model, vibration dynamic analysis, parameter optimization, single objective optimization, rigid body

Contents

Preface

This master project was done in an Erasmus exchange semester between Universiät Karlsruhe (Karlsruhe University, Germany) and Chalmers University of Technology (Sweden). The work that resulted in this thesis was done between August 2008 and January 2009 on the Department of Applied Mechanics, Division of Dynamics, Chalmers University of Technology.

This project is part of the research about vibration isolation in commercial vehicles by dint of advanced engine mounting systems.

I want to thank my supervisor and examiner of this project Professor Viktor Berbyuk for the possibility to write this thesis here in Göteborg and the assistance and guidance he gave me during this half year.

I also want to thank Hoda Yarmohamadi for her advice with modelling the vehicle and Thomas Nygårds for his help with Adams View. Both of them are PhD students at the Department of Applied Mechanics.

Göteborg January 2009

Felix Göbel

1 Introduction

One of the biggest challenges today's automotive development is faced with is lowering the fuel consumption of the vehicles. One obvious way to increase the fuel efficiency of a motorcar is to reduce its mass. But reduced masses result in increasing problems with vibrations and the dynamical behaviour in general. More vibrations mean additional wear and worse comfort and the comfort is an important quality characteristic which can influence the customers purchase decision.

One of the main sources of vibrations in vehicles is the engine. The engine excites vibrations because of the reciprocating masses like pistons and con-rods and the oscillating torque in the drive shaft.

The engine is connected to the chassis by engine mounts. The functions of the engine mounting system are supporting the engine on its location in the chassis, isolating the chassis from vibrations caused by the engine and protecting the engine from shocks, excited by the bumpiness of the road [2].

The dynamic excitations caused by the engine and the kinematic excitations caused by the road are changing in a broad range [2]. Therefore a mounting system with constant properties must always be a trade off between optimal settings for special sets of excitations.

Due to that it is expectable that an adaptive mounting system which is able to tune its properties to an optimum for each state of operation will lead to improved vibration isolation.

There are several concepts for active or semi-active engine mounts. Active mounts are often implemented as piezo-electric or magneto-electric actuators. Semi-active mounts are mostly hydraulic either with an adjustable bypass valve or with an electro- or magneto-rheological fluid [5] [6]. Or they utilize the depression of the intake manifold [7].

Semi-active mounting systems are available for passenger vehicles now but the application in commercial vehicles is quite different because of the larger weight of the engines used there and the stronger excitations with lower frequencies caused by diesel engines compared to the gasoline engines often used in passenger cars. In commercial vehicles conventional elastomeric or hydraulic mounts are in use until now.

In this thesis the SI unit system is used for all quantities.

1.1 Aim of the thesis

The overall goal of this project is the improvement of the comfort for the driver of a ground vehicle by dint of adaptive engine mounts. The steps in this direction which shall be done here are the development of a model which allows simulating the vibration dynamics of a vehicle under various excitations and with different adjustments of the mounting system. This model shall be simple enough to use it for parameter optimization and control engineering but complex enough to get significant results. Additionally requirements are the possibility to find optimal settings for an adaptive mounting system and to make predictions about the quantity of the improvement of comfort achievable thereby.

1.2 Former research

Beside the above mentioned development of active and semi-active mounts some research has been done about engine mounts and the whole mounting system.

Ohadi and Maghsoodi [10] studied the vibration behaviour of an engine on nonlinear hydraulic engine mounts. Bayram and Ugun [2] developed a model to simulate the vibration dynamics of a commercial vehicle with conventional mounting system, taking into account dynamic and kinematic excitations. Yarmohamadi [4] studied a similar model but extended about nonlinear mounts and controlled actuators. Choi and Song [1] and Olsson [3] did research about semi-active respectively active mounting systems with focus on controls. Choi et al. [9] and Lee and Lee [8] investigated the dynamics of a prototype active engine mount and the second designed an adaptive controller.

2 Modelling

To describe the behaviour of any physical system a model is necessary. In this case the modelling can be divided in three steps. In the first, the creation of the mechanical model, the real system is split up into components which can be described mathematically. Important decisions, what to take into account and what to neglect must be made in this section. In the second, mathematic equations describing the mechanical model shall be found. The result of the third step is the computational model. This is an expedient device to predict the behaviour of the real vehicle.

2.1 Mechanical model

A four-wheeled ground vehicle is abstracted as a mechanical model. This mechanical model consists of rigid bodies for the chassis, the unsprung wheel masses and the engine, connected with springs and dampers for the tires, the suspension and the mounts. The mounts can have translational and rotational stiffness and damping in all three directions.

The system has 13 degrees of freedom. The translation of the four unsprung wheel masses in z-direction ($z_{u1}, z_{u2}, z_{u3}, z_{u4}$), the translation of the chassis in z-direction (z_c), the rotation of the chassis around the x-axis (roll, φ) and the y-axis (pitch, ϑ), the translation of the engine in all three directions (e_x, e_y, e_z) and the rotation of the engine around all three axes (x, roll, α; y, pitch, β; z, yaw, γ).

The vehicle is excited kinematically by the road and dynamically by forces and torques induced by the engine.

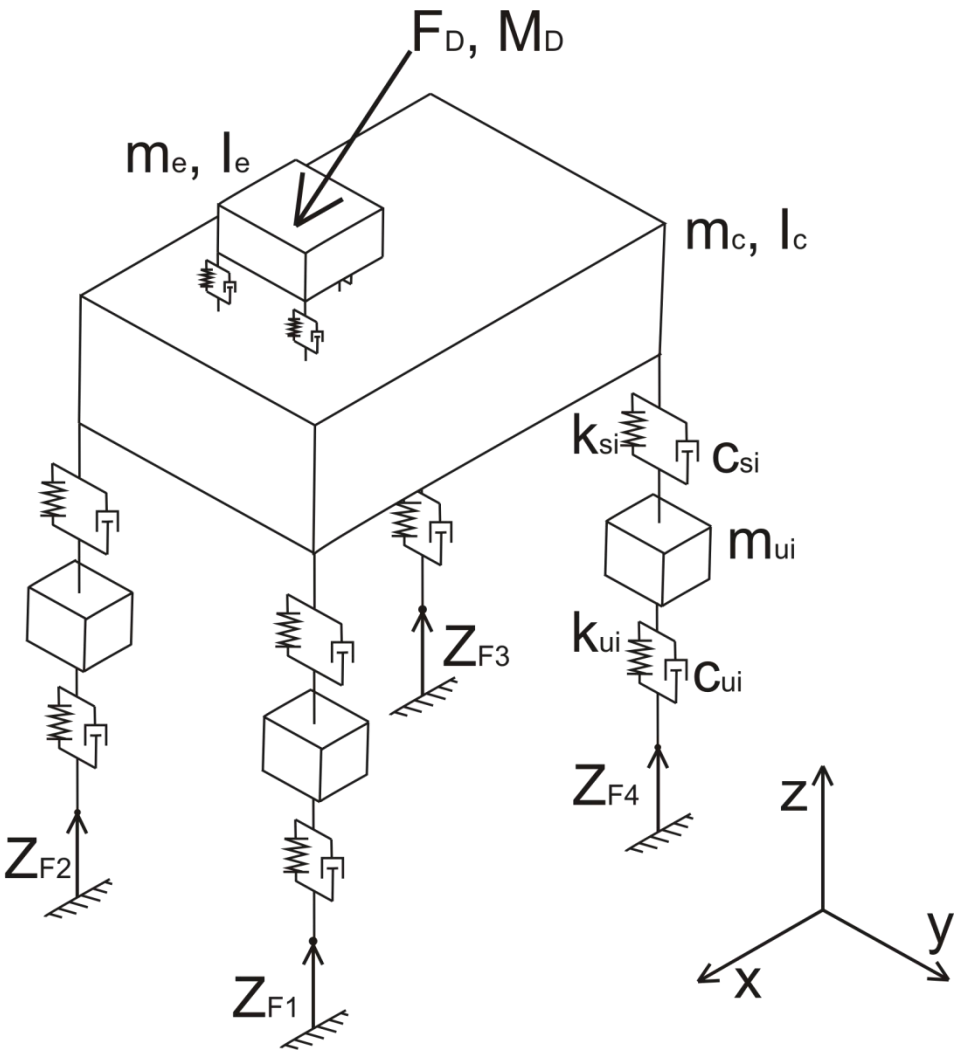

Figure 1: Mechanical model

All in all the following assumptions have been made:

- The chassis, engine and unsprung wheel masses are rigid bodies.
- The vehicle has only the above specified 13 degrees of freedom.
- The stiffness and damping of each mount are concentrated in one point.
- The mounts consist of linear springs and dampers in parallel.
- The mounts are the only connection between engine and chassis influencing the dynamic behaviour of the vehicle.
- The suspension and the tires consist of one dimensional linear springs and dampers in parallel.
- From the outside the vehicle is only influenced by gravity and the dynamic and kinematic excitations. That means no inertia forces caused by accelerations or cornering.

Those assumptions are necessary to reduce the computing time. And they enable easier understanding of the dynamic behaviour. Since there are intentions to use this

model for control engineering it is necessary to keep the complexity on a low level. The main restriction made here is probably the neglect of the elasticity of the chassis. But since the consideration of the chassis elasticity would increase the complexity of the model much, this is a good trade of for a simple model which still allows realistic predictions.

2.2 Mathematical model

The mechanical model can be mathematically described as follows:

Equilibrium of torques for the chassis:

$$\begin{bmatrix}1 & 0 & 0\\ 0 & 1 & 0\\ 0 & 0 & 0\end{bmatrix}\tilde{\tilde{I}}_c\,\ddot{\tilde{\Theta}} = \begin{bmatrix}1 & 0 & 0\\ 0 & 1 & 0\\ 0 & 0 & 0\end{bmatrix}\left[\sum_{i=1}^{4}\tilde{r}_{si}\times\tilde{F}_{si} - \sum_{j=1}^{3}\tilde{r}_{cj}\times\tilde{F}_{ej} - \sum_{j=1}^{3}\tilde{T}_{ej}\right]$$

Equilibrium of forces for the chassis:

$$m_c\,\ddot{z}_c = \left[\sum_{i=1}^{4}\tilde{F}_{si} - \sum_{j=1}^{3}\tilde{F}_{ej}\right]\cdot\tilde{e}_z - m_c\,g$$

Equilibrium of forces for the unsprung wheel masses:

$$m_{ui}\,\ddot{z}_{ui} = -F_{si} + k_{ui}(z_{Fi} - z_{ui}) + c_{ui}(\dot{z}_{Fi} - \dot{z}_{ui}) - m_{ui}\,g$$

Equilibrium of forces for the engine:

$$m_e\,\ddot{\tilde{e}} = \tilde{F}_D + \sum_{j=1}^{3}\tilde{F}_{ej} - m_e\,\tilde{g}$$

Equilibrium of torques for the engine:

$$\tilde{\tilde{I}}_e\ddot{\tilde{\Phi}} = \tilde{M}_D + \sum_{j=1}^{3}\tilde{r}_{ej}\times\tilde{F}_{ej} + \sum_{j=1}^{3}\tilde{T}_{ej}$$

$$\tilde{F}_{ej} = \tilde{\tilde{K}}_{ej}\left(\tilde{\Theta}\times\tilde{r}_{cj} - \tilde{\Phi}\times\tilde{r}_{ej}\right) + \tilde{\tilde{C}}_{ej}\left(\dot{\tilde{\Theta}}\times\tilde{r}_{cj} - \dot{\tilde{\Phi}}\times\tilde{r}_{ej}\right)$$

$$F_{si} = k_{si}(z_{ui} - z_{si}) + c_{si}(\dot{z}_{ui} - \dot{z}_{si})$$

$$\tilde{T}_{ej} = \tilde{\tilde{K}}_{etj}\left(\tilde{\Theta} - \tilde{\Phi}\right) + \tilde{\tilde{C}}_{etj}\left(\dot{\tilde{\Theta}} - \dot{\tilde{\Phi}}\right)$$

$$z_{si} = z_c + \left(\tilde{\Theta}\times\tilde{r}_{si}\right)\cdot\tilde{e}_z$$

Initial conditions:

The initial state of the system is the static equilibrium.

Notations

Tensors

$\tilde{\tilde{C}}_{ej}$ Translational damping tensor of the j*th* mount w.r.t the global co-ordinate system

$\tilde{\tilde{C}}_{etj}$ Rotational damping tensor of the j*th* mount w.r.t the global co-ordinate system

$\tilde{\tilde{I}}_{c}$ Inertial tensor of the chassis

$\tilde{\tilde{I}}_{e}$ Inertial tensor of the engine

$\tilde{\tilde{K}}_{ej}$ Translational stiffness tensor of the j*th* mount w.r.t the global co-ordinate system

$\tilde{\tilde{K}}_{etj}$ Rotational stiffness tensor of the j*th* mount w.r.t the global co-ordinate system

Vectors

$\tilde{\Theta} = \begin{pmatrix} \varphi \\ \vartheta \\ \psi \end{pmatrix}$ Rotation of the chassis w.r.t the global co-ordinate system

φ Roll (rotation around the x-axis) (degree of freedom)

ϑ Pitch (rotation around the y-axis) (degree of freedom)

$\psi = 0$

$\tilde{\Phi} = \begin{pmatrix} \alpha \\ \beta \\ \gamma \end{pmatrix}$ Rotation of the engine w.r.t the global co-ordinate system

α Roll (rotation around the x-axis) (degree of freedom)

β Pitch (rotation around the y-axis) (degree of freedom)

γ Yaw (rotation around the z-axis) (degree of freedom)

$\tilde{F}_{D}$ Dynamic excitation force acting on the CM of the engine

$\tilde{F}_{ej}$ Force of the j*th* mount

$\tilde{F}_{si}$ Force of the i*th* suspension

$\tilde{M}_{D}$ Dynamic excitation Torque acting on the CM of the engine

$\tilde{T}_{ej}$ Torque of the j*th* mount

$\tilde{e}$ Position of the CM of the engine w.r.t. global co-ordinates (3 degrees of freedom)

$\tilde{e}_z$ Unit vector in z-direction in the global co-ordinates

$\tilde{g}$ Gravity

$\tilde{r}_{cj}$ Position of the j*th* mount w.r.t. the CM of the chassis

$\tilde{r}_{ej}$ Position of the j*th* mount w.r.t. the CM of the engine

$\tilde{r}_{si}$ Position of the i*th* suspension w.r.t. the CM of the chassis

Scalars

$F_{si} = \tilde{F}_{si} \cdot \tilde{e}_z$ z-component of the force of the i*th* suspension

c_{si} Damping of the i*th* suspension

c_{ui} Damping of the i*th* tire

$g = \tilde{g} \cdot \tilde{e}_z$ Gravity

k_{si} Stiffness of the i*th* suspension

k_{ui} Stiffness of the i*th* tire

m_c Mass of the chassis

m_e Mass of the engine

m_{ui} Mass of the i*th* unsprung wheel mass

z_c Position of the CM of the chassis in z-direction w.r.t. global co-ordinates (degree of freedom)

z_{Fi} Kinematic excitation of the i*th* tire in z-direction

z_{si} Displacement of the chassis at the i*th* suspension in z-direction

z_{ui} Position of the i*th* unsprung wheel mass in z-direction (degree of freedom)

2.3 Computational model

The computational model is created in MSC Adams View. The Adams Model corresponds to the mechanical model with 13 degrees of freedom.

Adams View as a simulation tool has some advantages:

- The modelling process is clear and straightforward.
- The plausibility of the results can be checked visually in the animated simulation mode.
- A powerful postprocessor exists.
- An optimization tool exists.

But also a few disadvantages:

- There are probably faster tools.
- The implementation of controls is limited.
- The build in optimizer allows only single objective optimizations.

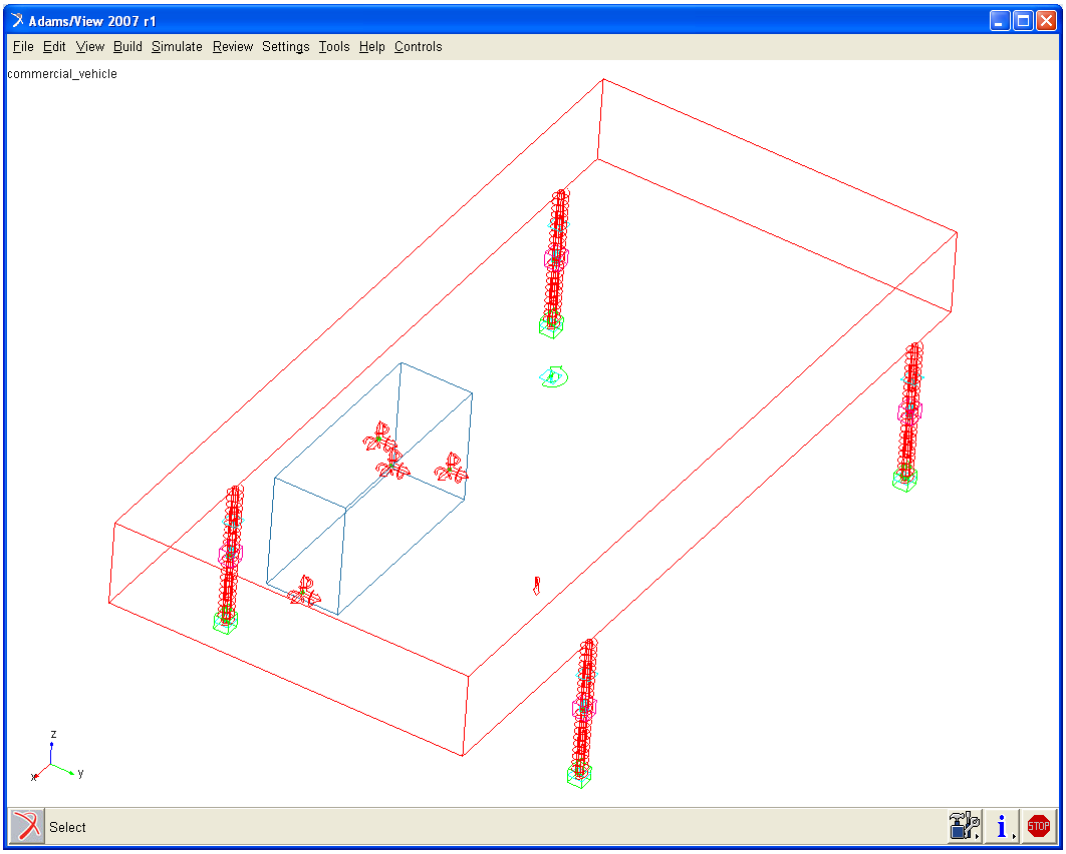

Figure 2: The Adams model

The chassis is connected to the ground with a joint that allows translational motion in global z-direction and rotation around the x- and y-axis. The motion of the parts at the bottom of the wheels is free in x- and y-direction, in z-direction it is controlled by the kinematic excitations. The springs of the suspension and tires are always vertical. The mounts, connecting engine and chassis are modelled with three six component forces and another six component force is acting on the centre of mass of the engine for the dynamic excitations.

A more detailed description of the Adams model exists in the appendix (chapter 8.1.).

2.3.1 Capabilities of the Adams model

This model gives the possibility to simulate the behaviour of the vehicle under different excitations. The dynamic excitations can represent different kinds of engines, running with different speeds and generating different torques. The kinematic excitations can represent different road conditions and driving speeds. Since the model is completely parameterized it is easily possible to modify it. This allows using it to simulate all four-wheel ground vehicles.

All parameters describing the model like geometry, mass, inertia, stiffness, damping and the time dependent excitations are needed as inputs.

As results the motions in all degrees of freedom, all forces or other measurable quantities can be obtained, either as run time function or rated with operators like RMS (root mean square) or MAX (maximum).

If required some extensions can easily be made in the Adams model:

- The mount forces can be described by any function of time, mount deflections or other measurable quantities.
- Inertia forces due to accelerations can be added.
- Other setups than three point mounting systems can be modelled.

3 Verification

To verify the model several experiments have been simulated. Special settings of parameters and excitations were chosen which allow a prediction of the response of the system at least qualitatively. Some of the degrees of freedom are locked so that the behaviour in the remaining can be comprehended in a better way.

The appendix provides more details (chapter 8.2.).

Résumé of verification:

The Adams model is not unstable or diverging for realistic sets of input. It is able to represent the mechanical model, as long as the forces in the suspensions and tires are not too large. If the springs representing the suspensions and tires are compressed to length zero, they flip and the behaviour of the system gets inaccurate. But because the length of both springs is 0.5 m at the static equilibrium, this cannot happen under realistic circumstances.

4 Statement of the vibration dynamics problem

To determine the behaviour of the system a dynamic problem has to be solved.

Dynamic problems can be classified in three different categories:

I. Inverse dynamic problems

   The motions of a system are known and the forces acting on it shall be calculated.

II. Direct dynamic problems

   The forces acting on a system and its initial state are known and the motions shall be calculated.

III. Semi-inverse dynamic problems

   Some of the motions or some kinematic constraints and some of the forces are known and the missing motions and forces shall be calculated. That means the semi-inverse dynamic problem is the most general one and includes the two others as special cases.

The first ones are the easiest to solve. Since the positions $x(t)$ are known the accelerations $\ddot{x}(t)$ can easily be calculated by derivation and Newton's second law $\tilde{F} = m\ddot{\tilde{x}}$ can be solved.

The solution of problems of the second kind can be more difficult because the accelerations given by Newton's second law must be integrated two times to get the motions. And integration can be much more difficult than derivation.

The third problems are the most general ones and the most difficult ones to solve. A set of constraints and differential equations with initial conditions has to be solved. If there are not enough known constraints, there is no unique solution.

Vibration dynamics means, the system performs motions about a static equilibrium, in our case with relative low-amplitudes and high-frequencies. If the system behaves linear and it is excited harmonic, these motions are the superposition of harmonic oscillations.

The vibration dynamics problem worked on in this thesis is semi-inverse. Some forces which are acting on the system like the dynamic excitations and weight-forces are known and there are a lot of kinematic constraints like the kinematic excitations and restrictions of motion described by the joints in the mechanical model.

A general dynamic problem can mathematically be specified as follows.

$$\dot{\tilde{x}}(t) = f(\tilde{x}(t), \tilde{p}, \tilde{d}, \tilde{U}(t, \tilde{x}), \tilde{f}(t))$$

$$\tilde{x}(0) = \tilde{x}_0$$

With:

$\tilde{x}(t)$	State vector
$\tilde{p}$	System parameters
$\tilde{d}$	Design parameters

$\tilde{U}(t, \tilde{x})$	Control vector
$\tilde{f}(t)$	Excitations
$\tilde{x}_0$	Initial conditions

In our mechanical case, the state vector contains the positions and velocities of the bodies in all 13 degrees of freedom. System parameters are all properties of the vehicle which cannot be modified, like the geometry, mass, inertia and the given stiffness and damping. Design parameters are the properties of the mounts which get changed to optimize the dynamic behaviour. The control vector includes the actuating forces so they exist. The excitations are the forces and torques caused by the operating engine (dynamic excitations) and the motions of the wheel bases caused by the roughness of the road (kinematic excitations).

4.1 General problem 1 (The conventional mounting system)

Since all properties of the commercial vehicle and the mounting system are know and the excitations are given, the behaviour of the system is determined by the equations given in chapter 2.2.

Known input:

- System and design parameters (chapter 8.3.)
- Dynamic excitations (chapter 5.1.2.1.)
- Kinematic excitations (chapter 5.1.2.2.)
- No active or controlled elements

Required output:

- Motions of the system in all 13 degrees of freedom ($\tilde{x}(t)$)
- Deflections of the mounts ($\widetilde{de}(t)$)
- Transmitted forces ($\tilde{F}_t(t)$)

The solution has to fulfil the mathematical model given by the equations in chapter 2.2 and the initial conditions which is the static equilibrium.

This problem can be solved, using the developed Adams model.

An example for this kind of problem is given in chapter 5.2.

4.2 General problem 2 (Optimization)

Determine the design parameters which minimize the objective function and fulfil the constraints given in chapter 5.3.1. Those design parameters must fit in some physical restrictions:

$$\tilde{d}^{min} < \tilde{d} < \tilde{d}^{max}$$

That means the solution of this problem is a set of design-parameters $\hat{\tilde{d}}$ which minimize $g = g(\tilde{x}(t), \widetilde{de}(t), \tilde{F}_t(t))$ with respect to the appropriated constraints.

An example for this kind of problem is given in chapter 5.3.

5 Simulation

A few examples of simulations to show the capabilities of the model shall be presented.

5.1 Input

The Adams model needs all parameters, the dynamic and kinematic excitations as input.

5.1.1 Parameters

The values of the parameters are the properties of a commercial vehicle.

Mass of the chassis: $m_c = 8000$ kg

Mass of the engine: $m_e = 1900$ kg

Wheel track: $(\tilde{r}_{s1})_y - (\tilde{r}_{s2})_y = (\tilde{r}_{s4})_y - (\tilde{r}_{s3})_y = 2.49$ m

Wheel base: $(\tilde{r}_{s1})_x - (\tilde{r}_{s4})_x = (\tilde{r}_{s2})_x - (\tilde{r}_{s3})_x = 3.6$ m

The engine is mounted on a three point mounting system with one front mount and two symmetric rear mounts.

The remaining parameters exist in the appendix (chapter 8.3.).

5.1.2 Excitations

5.1.2.1 Dynamic excitations

The dynamic excitations are the forces and torques caused by the operation of the engine. For different operating conditions of the engine, they are mathematically described as follows:

Dynamic excitation 1: Driving with constant high engine speed

$$F_x = 30 \sin(\omega t)$$

$$F_y = 250 \sin(\omega t)$$

$$F_z = 250 \sin(\omega t)$$

$$M_x = 300 \sin(\omega t)$$

$$M_y = 100 \sin(\omega t)$$

$$M_z = 100 \sin(\omega t)$$

With: $\omega = 300 \frac{1}{s}$; $f = \frac{\omega}{2\pi} \frac{1}{s} = \frac{300}{2\pi} \frac{1}{s} = 47.75 \text{ Hz} = 2865 \frac{1}{\text{min}}$

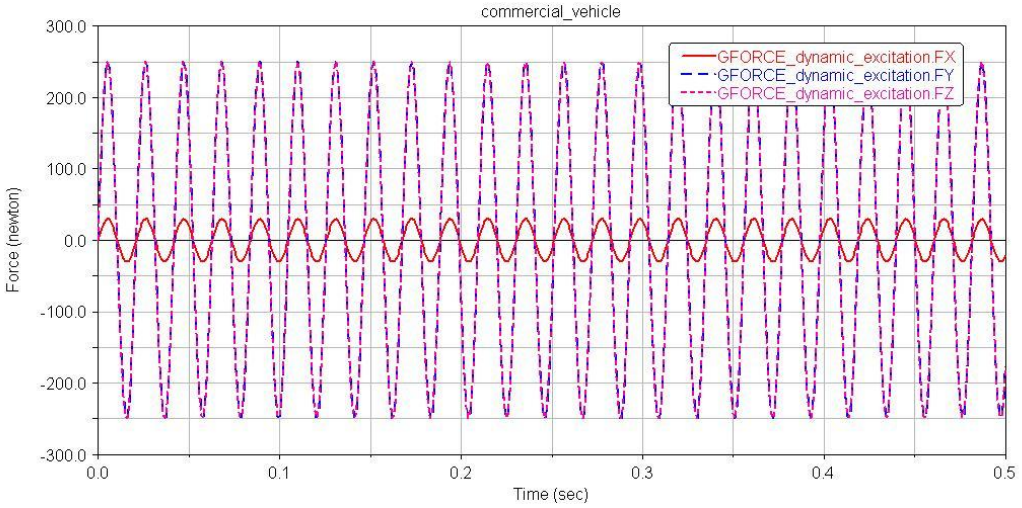

Figure 3: High frequency – low amplitude forces exciting the engine.

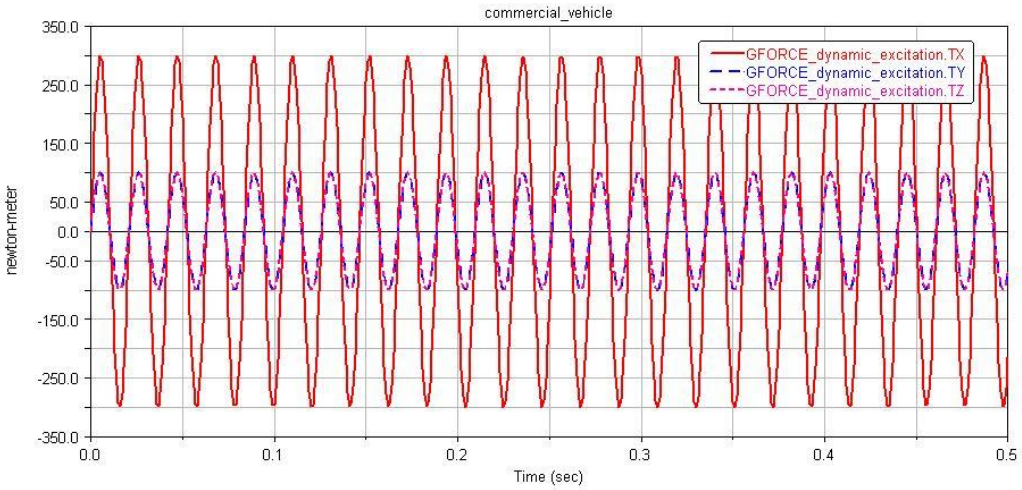

Figure 4: High frequency – low amplitude torques exciting the engine.

Dynamic excitation 2: Driving with constant low engine speed

$$F_x = 60 \sin(\omega t)$$

$$F_y = 600 \sin(\omega t)$$

$$F_z = 600 \sin(\omega t)$$

$$M_x = 800 \sin(\omega t)$$

$$M_y = 200 \sin(\omega t)$$

$$M_z = 200 \sin(\omega t)$$

With: $\omega_1 = 150 \frac{1}{s}$; $f = \frac{\omega}{2\pi} \frac{1}{s} = \frac{200}{2\pi} \frac{1}{s} = 23.87 \text{ Hz} = 1432 \frac{1}{\text{min}}$

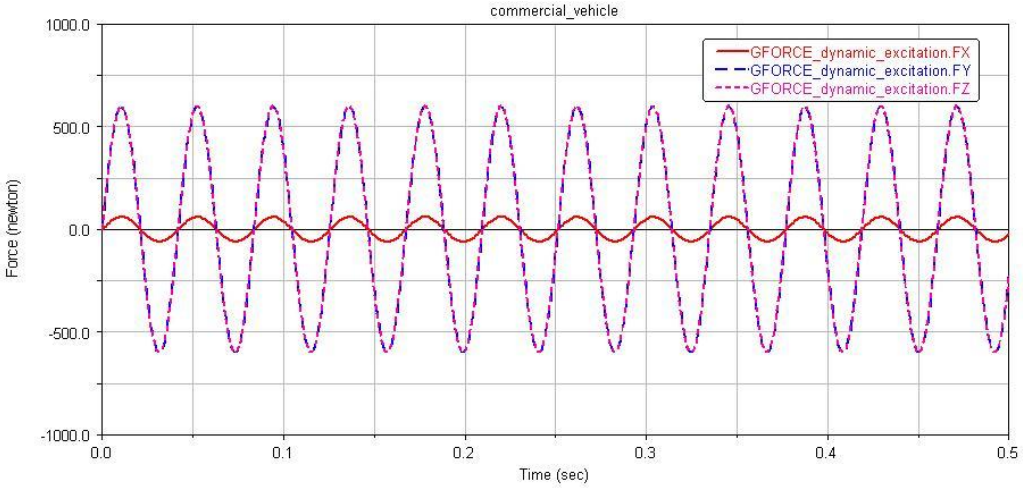

Figure 5: Low frequency – high amplitude forces exciting the engine.

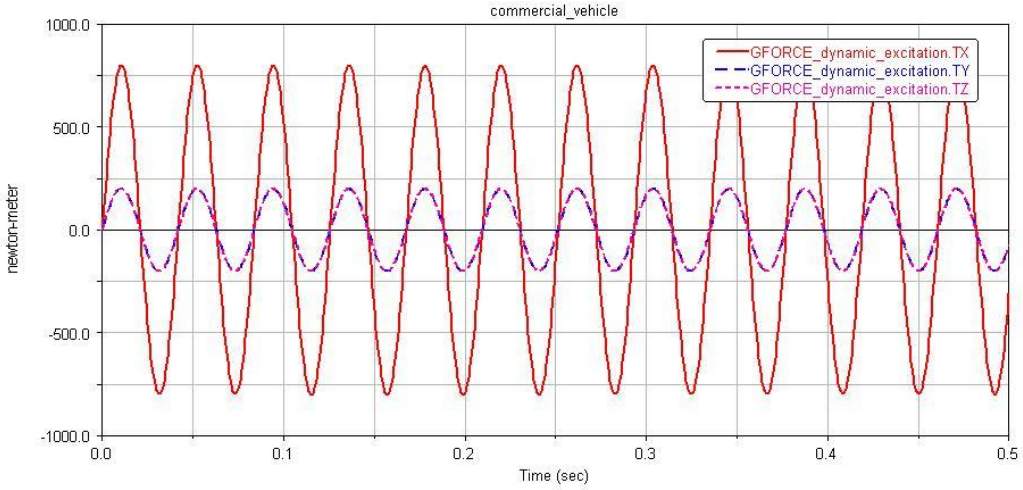

Figure 6: Low frequency – high amplitude torques exciting the engine.

Dynamic excitation 3: Turning on the engine

$$F_x = \begin{cases} \left(1 - \frac{1}{5}\,t\right) 100 \sin(\omega_2^* t^2 + \omega_1^* t)\,; \text{for } 0 < t < 2 \\ \frac{3}{5} 100 \sin(\omega_3 t)\,; \text{for } 2 \le t < 3 \end{cases}$$

$$F_y = \begin{cases} \left(1 - \frac{1}{5}\,t\right) 1000 \sin(\omega_2^* t^2 + \omega_1^* t)\,; \text{for } 0 < t < 2 \\ \frac{3}{5} 1000 \sin(\omega_3 t)\,; \text{for } 2 \le t < 3 \end{cases}$$

$$F_z = \begin{cases} \left(1 - \frac{1}{5}\,t\right) 1000 \sin(\omega_2^* t^2 + \omega_1^* t)\,; \text{for } 0 < t < 2 \\ \frac{3}{5} 1000 \sin(\omega_3 t)\,; \text{for } 2 \le t < 3 \end{cases}$$

$$M_x = \begin{cases} \left(1 - \frac{1}{6}\,t\right) 1200 \sin(\omega_2^* t^2 + \omega_1^* t)\,; \text{for } 0 < t < 2 \\ \frac{2}{3} 1200 \sin(\omega_3 t)\,; \text{for } 2 \le t < 3 \end{cases}$$

$$M_y = \begin{cases} \left(1 - \frac{1}{4}\,t\right) 400 \sin(\omega_2^* t^2 + \omega_1^* t)\,; \text{for } 0 < t < 2 \\ \frac{1}{2} 400 \sin(\omega_3 t)\,; \text{for } 2 \le t < 3 \end{cases}$$

$$M_z = \begin{cases} \left(1 - \frac{1}{4}\,t\right) 400 \sin(\omega_2^* t^2 + \omega_1^* t)\,; \text{for } 0 < t < 2 \\ \frac{1}{2} 400 \sin(\omega_3 t)\,; \text{for } 2 \le t < 3 \end{cases}$$

With:

$$\omega_1^* = 4\,\frac{1}{s}\;;\; \omega_2^* = 23\,\frac{1}{s}\;;\; \omega_3 = 100\frac{1}{s} \Rightarrow f_3 = \frac{\omega_3}{2\,\pi}\frac{1}{s} = \frac{100}{2\,\pi}\frac{1}{s} = 15.92\text{ Hz} = 955\,\frac{1}{\text{min}}$$

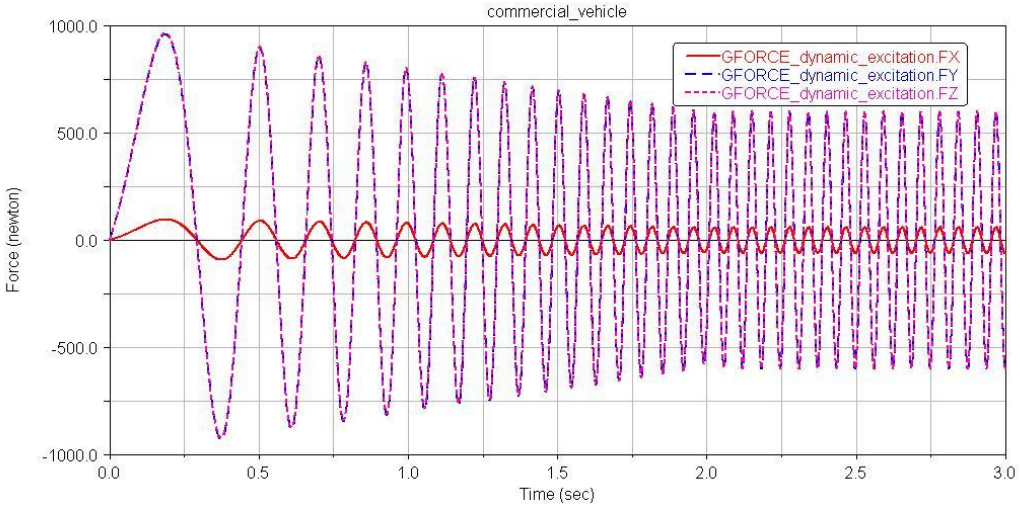

Figure 7: Forces exciting the engine during the start and running with idle speed.

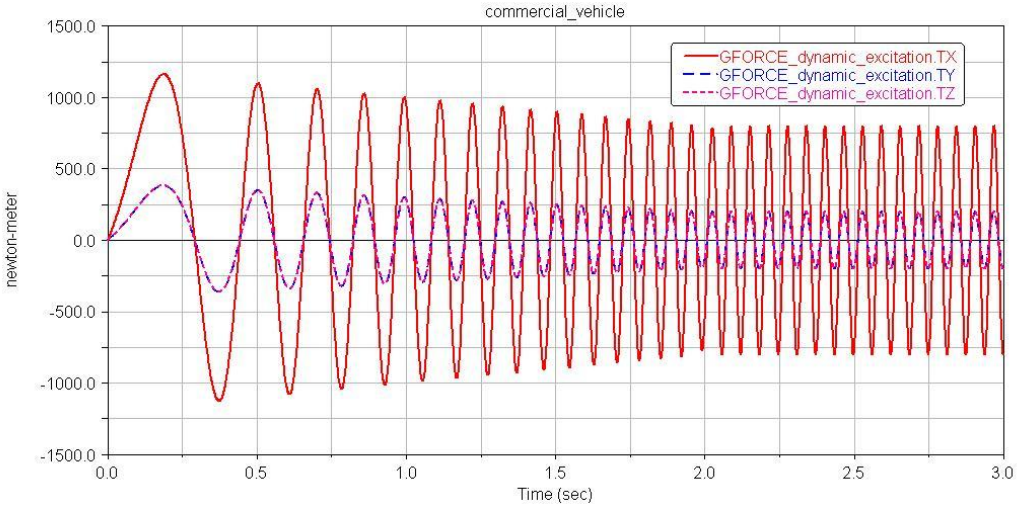

Figure 8: Torques exciting the engine during the start and running with idle speed.

5.1.2.2 Kinematic excitations

The kinematic excitations are the displacement of the wheel bases caused by a bump on the road. For different conditions of the road, they are mathematically described as follows:

$z_{Ffl} = 0$

$z_{Ffr} = h\ step(time, t_0 - \Delta\tau, 0, t_0, 1)\ step(time, t_0 + \Delta t, 1, t_0 + \Delta t + \Delta\tau, 0)$

$z_{Frr} = h\ step(time, t_0 - \Delta\tau + \Delta T, 0, t_0 + \Delta T, 1)\ step(time, t_0 + \Delta T + \Delta t, 1, t_0 + \Delta T + \Delta t + \Delta\tau, 0)$

$z_{Frl} = 0$

$z_{Ffl};\ z_{Ffr};\ z_{Frr};\ z_{Frl}$ Displacement of the wheel base front left; front right; rear right; rear left.

The *step* function in Adams approximates a discontinuous step as a smooth function.

Kinematic excitations 1: Driving with low speed on a bad road ($v = 36 \frac{km}{h}$)

$h = 0.05$	Height of the bump
$t_0 = 0.9$	Time when the front wheel arrives on top of the bump
$\Delta\tau = 0.02$	Time the wheel needs to roll onto the bump
$\Delta t = 0.03$	Time the wheel needs to cross the bump
$\Delta T = 0.36$	Time delay between the front and rear wheel

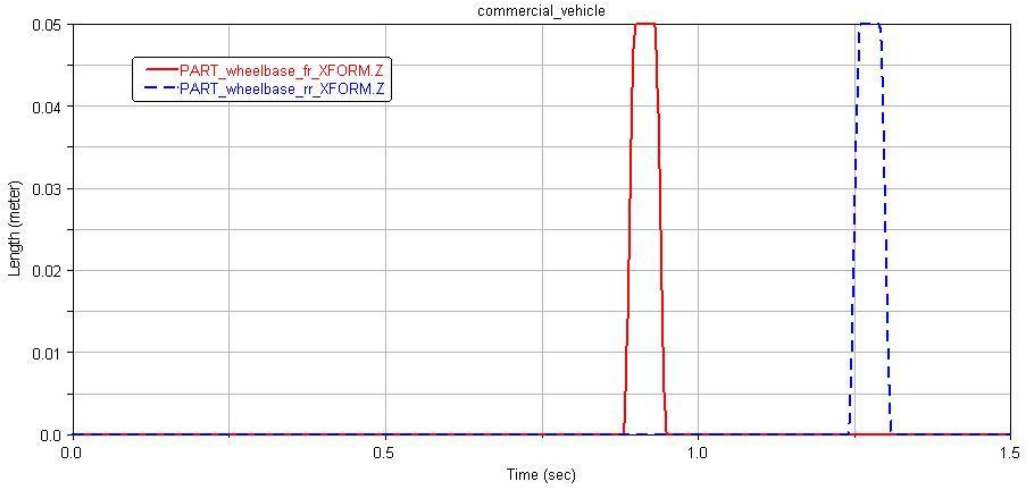

Figure 9: Kinematic excitations of the front (—) and rear (- - -) right wheels.

Kinematic excitations 2: Driving with low speed on a good road ($v = 36\frac{km}{h}$):

$h = 0.005$	Height of the bump
$t_0 = 0.9$	Time when the front wheel arrives on top of the bump
$\Delta\tau = 0.006$	Time the wheel needs to roll onto the bump
$\Delta t = 0.03$	Time the wheel needs to cross the bump
$\Delta T = 0.36$	Time delay between the front and rear wheel

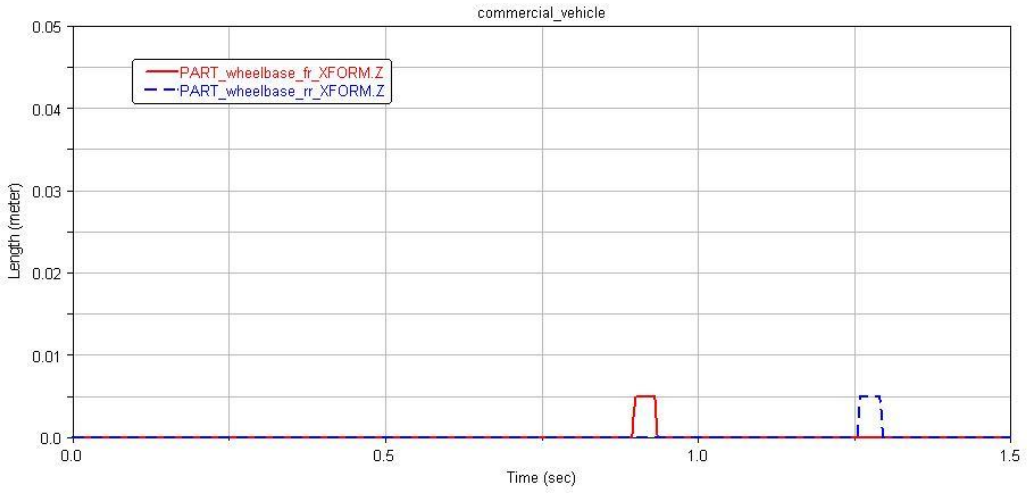

Figure 10: Kinematic excitations of the front (—) and rear (- - -) right wheels.

Kinematic excitations 3: Driving with high speed on a good road ($v = 90\frac{km}{h}$):

$h = 0.005$	Height of the bump
$t_0 = 0.9$	Time when the front wheel arrives on top of the bump
$\Delta\tau = 0.003$	Time the wheel needs to roll onto the bump

$\Delta t = 0.012$ Time the wheel needs to cross the bump

$\Delta T = 0.144$ Time delay between the front and rear wheel

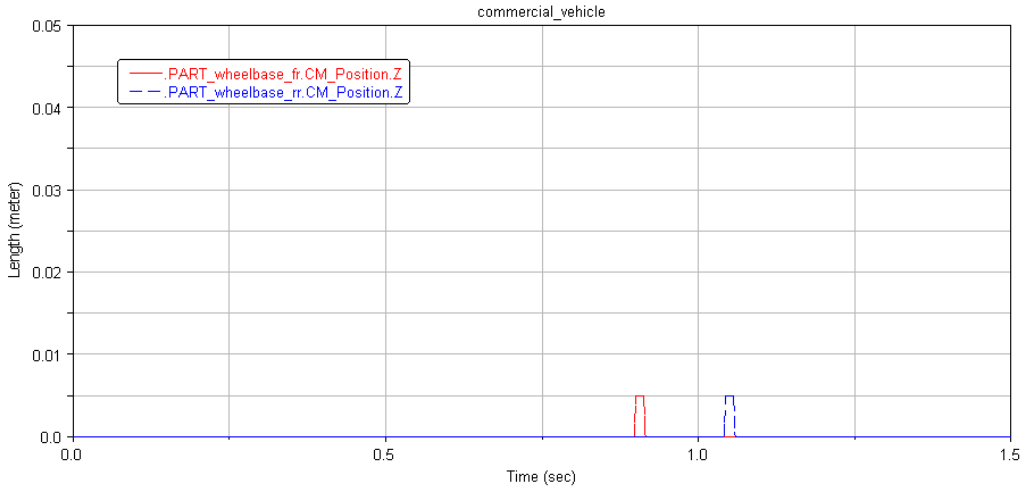

Figure 11: Kinematic excitations of the front (—) and rear (- - -) right wheels.

5.2 A single run

The vibration dynamics of a commercial vehicle with a total mass of 9900 kg and conventional mounting system are analysed. The vehicle is excited dynamically and kinematically. The engine is running with high rotational speed ($2865\ \frac{1}{\text{min}}$). The vehicle is driving with high speed ($90\ \frac{\text{km}}{\text{h}}$) on a good road.

The interesting outputs are the vibrations of the chassis, the deflections of the mounts and the sum of the forces transmitted by all three mounts.

5.2.1 Input

The model of a commercial vehicle is excited with the dynamic excitations 1 (high engine speed; chapter 5.1.2.1.) and kinematic excitations 3 (high speed, good road; chapter 5.1.2.2.). That means the dynamic excitations are harmonic with constant amplitude and frequency and the kinematic excitations start not before $t = 0.85$ s.

5.2.2 Results

The vibrations of the chassis can be described by the magnitude of the acceleration at the position of the driver's seat.

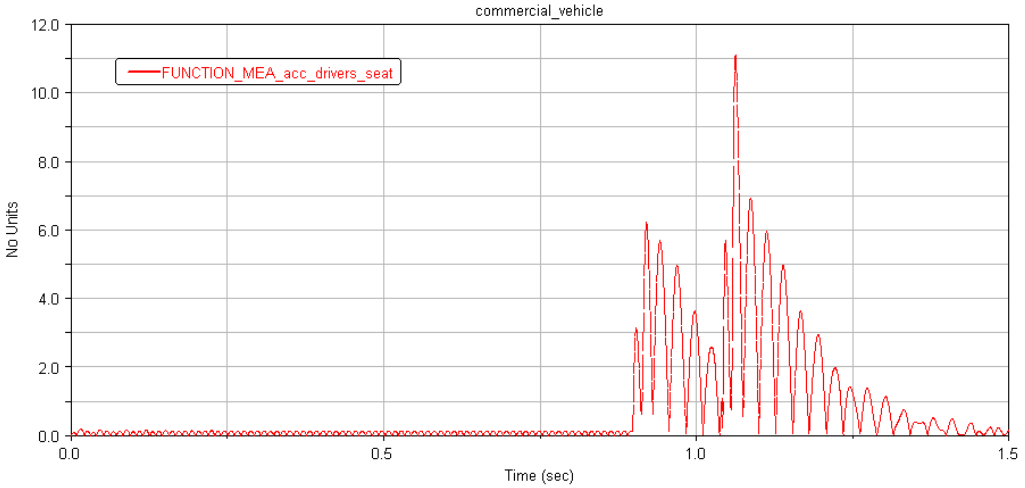

Figure 12: Magnitude of acceleration of the driver's seat

It is clearly visible, that the vibrations caused by the kinematic excitations are much bigger than those caused by the dynamic excitations, although the bump in the road is only 5 mm high.

The transmitted forces (here measured the magnitude of the vector sum of the three mount forces) are describing the load of the mounting system.

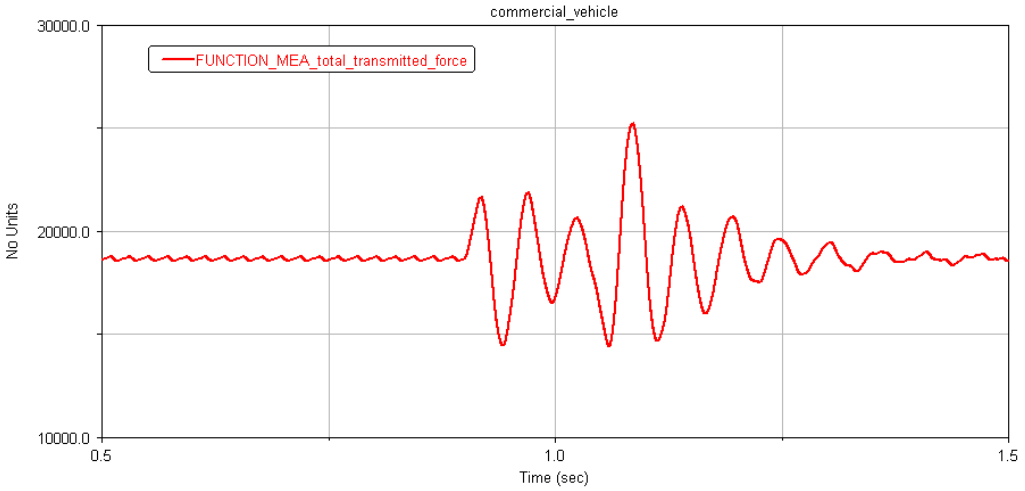

Figure 13: Total transmitted force

The transmitted forces are also dominated by the kinematic excitations. They are oscillating around the static weight of the engine.

The deflections of the mounts are important to know because any physical mount can only bear bordered deflections.

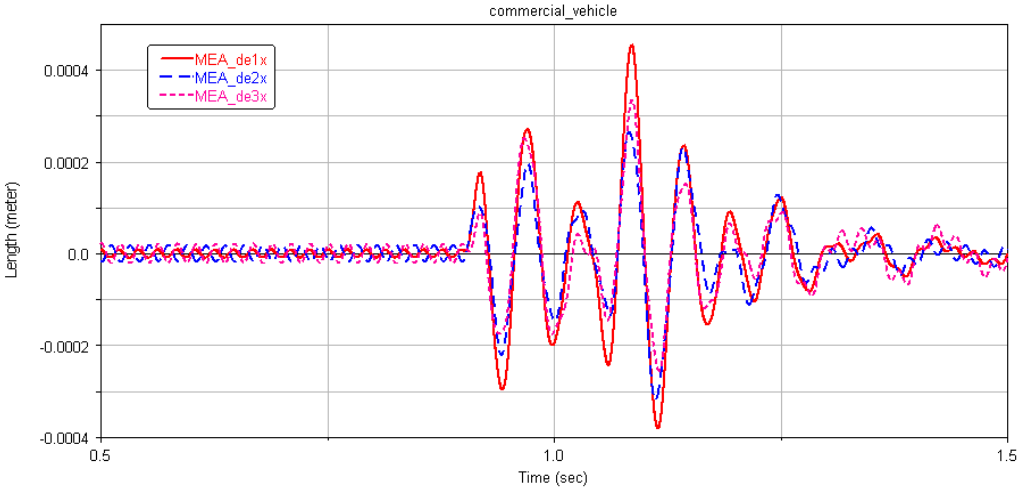

Figure 14: Mount deflections in x-direction

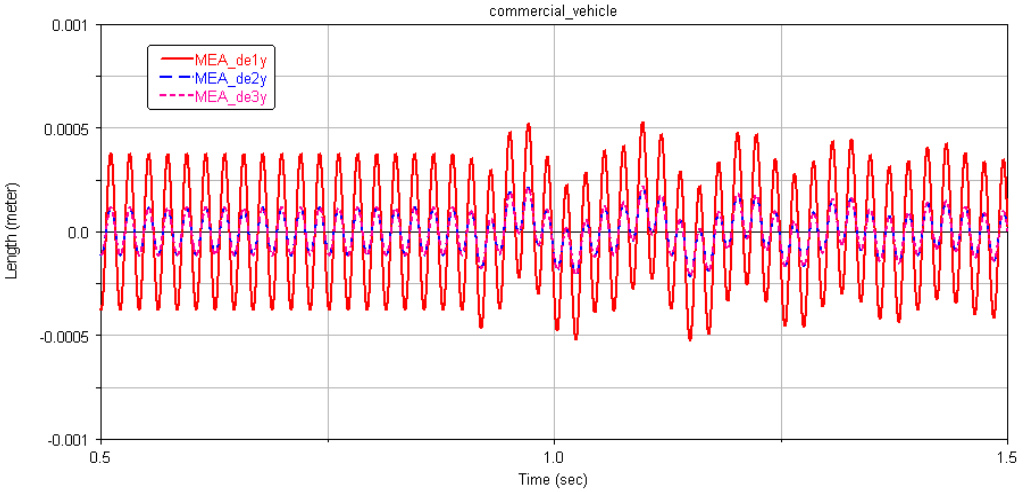

Figure 15: Mount deflections in y-direction

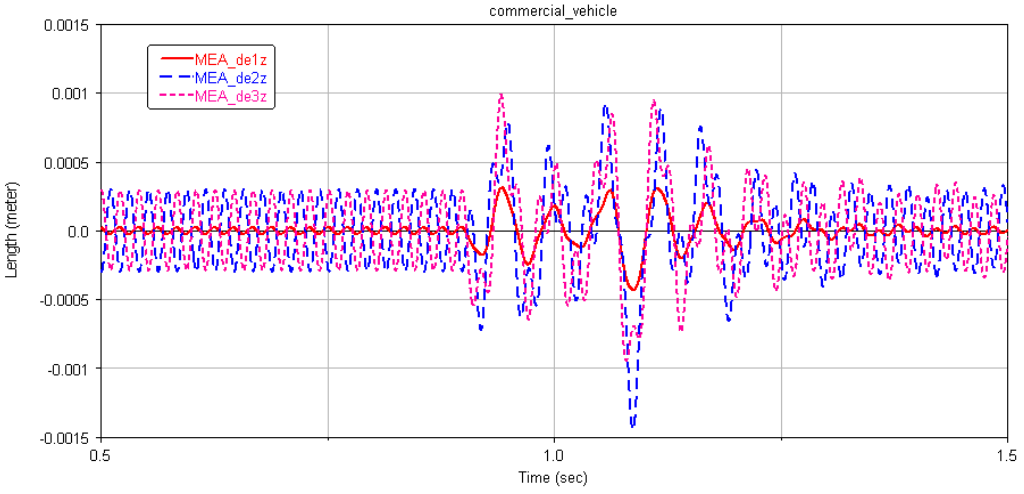

Figure 16: Mount deflections in z-direction

The mount deflections except those in y-direction are dominated by the kinematic excitations too. The front mount (mount number 1) is mainly deflected in y-direction. The rear mounts (number 2 and 3) are mainly deflected in z-direction. In the time span between 0.5 s and 0.85 s where only dynamic excitations are acting, the deflections of the rear mounts are of equal amplitude and in-phase in y-direction respectively in opposite phase in x- and z-direction. That is understandable because the mounting system and the dynamic excitations are symmetric about the cars longitudinal axis.

5.3 Optimization

The optimizer Adams is equipped with facilitates to find values for selected design variables which are optimal with respect to a scalar objective function and optionally a set of constraints.

Optimal settings for a mounting system which is able to switch some of its parameters between constant values depending on the operating conditions (state of street and engine) can be found with this method.

Since the comfort of the vehicle shall be improved it is assumable that the translational and rotational displacements, velocities and accelerations of the chassis are a rate for the vibrations. Out of those three the accelerations are the quantity which describes the disturbance caused by the vibrations best, because the accelerations are proportional to the forces the driver senses as unpleasant. That means a functional of the accelerations of the chassis can be used as a criterion for the comfort of the vehicle.

Beside this the total transmitted force and the deflections of the mounts must not be larger than a defined threshold to protect the engine, drive train and the mounts against damage. The deflections of the mounts are determined by the rotational and translational displacement of the engine and chassis.

All those quantities are oscillating. Due to that they have to be assessed in some way. This can be done by dint of the root-mean-square (RMS) or the maximum (MAX). The RMS has the advantage that it is not dominated by one value but takes into account all values during the whole time span.

Since the vibrations of the chassis which are caused by kinematic excitations cannot be influenced by the mounting system in a predictable way, it is not useful to take them into account for calculation of the criterion. But the kinematic excitations cause transmitted forces and mount deflections, which are not allowed to exceed defined thresholds.

To reach that it is necessary to have only dynamic excitations in the beginning of the simulation and start the kinematic excitations at a specified time. In the beginning of the simulation there are most likely some transient oscillations which are not realistic. For the criterion only the time span between the end of transient oscillations and the

start of the kinematic excitations has any significance. But the constraints have to be fulfilled for the whole time starting from the end of the transient oscillations.

To reach that the simulation running in the optimization loop consists of three sections:

1. $t = 0 \ldots 0.5$ s

   Only dynamic excitations are acting. For a short period of time there are transient oscillations because the simulation starts from the static equilibrium. This period has no physical meaning in the simulation of steady state operating conditions.

2. $t = 0.5 \ldots 0.85$ s

   Only dynamic excitations are acting. The system is oscillating in a steady state.

3. $t = 0.85 \ldots 1.5$ s

   Kinematic and dynamic excitations are acting. The kinematic excitations have much more influence on the vibrations than the dynamic.

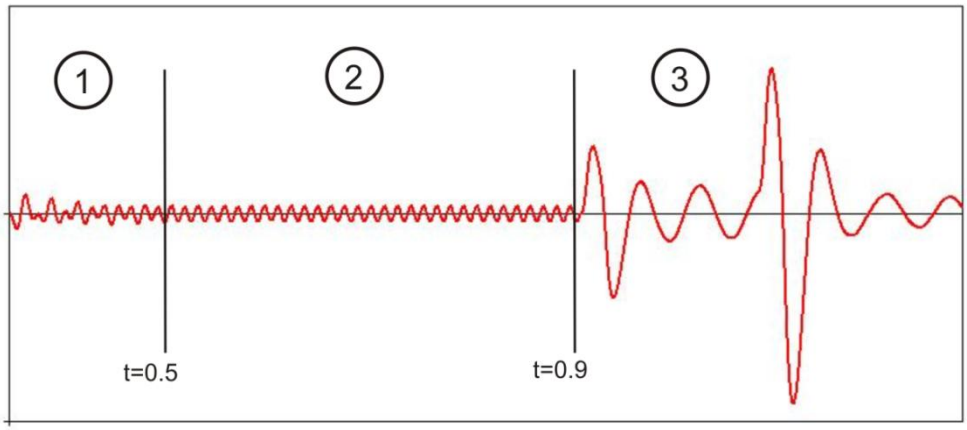

Figure 17: The three parts of vibration time history

The objective is calculated only during part two. The constraints have to be fulfilled during part two and three.

An exception of this consideration is the simulation of starting the engine. Here are no unrealistic transient oscillations and as long as the vehicle is standing still no kinematic excitations.

5.3.1 Objective function, design variables and constraints

The vibrations of the vehicle shall be reduced to improve the comfort. As mentioned above the acceleration of a point of the chassis located at the position of the driver's seat is a good rate for the disturbance of the vibrations. Those accelerations are averaged over time by the root-mean-square.

Objective: $g = \sqrt{\frac{1}{|t_2 - t_1|}\int_{t_1}^{t_2} \left\|\ddot{\tilde{s}}(t)\right\|^2 dt}$

g shall be minimized.

g Objective function

$\ddot{\tilde{s}}(t)$ Acceleration of a point of the chassis, located at the position of the driver's seat

t Simulation time

t_1 Start of the time span during which the objective is calculated

t_2 End of the time span during which the objective is calculated

$\|\tilde{x}\|$ The Euclidean norm of $\tilde{x}$

Design parameters are the parameters for which optimal values shall be found. Here the design parameters are the damping of the front mount in y- (lateral) and of the rear mounts in z-direction.

Those directions are chosen since the deflections of the mounts are the biggest there.

The damping is chosen since most existing solutions for semi-active engine mounts can vary the damping. For example by switching a hydraulic bypass valve or changing the viscosity of a magneto- or electro-rheological fluid.

Design parameters: $Ce1yy, Ce2zz = Ce3zz$

Ceijk jk element of the translational damping tensor of the i*th* mount.

The constraints of the optimization result from the restrictions of mount deflections and transmitted forces mentioned above.

Constraints:

$$|deix|, |deiy|, |de1z| < 0.005\ ;\ |de2z|, |de3z| < 0.01\ ;\ \left\|\sum \tilde{F}ti\right\| < 72000$$

For: $i \in \{1,2,3\}$

deij Translational deflection of the i*th* mount in j*th*-direction

$\tilde{F}ti$ Transmitted force of the i*th* mount

The design variables are changing due to the optimization but they cannot imbibe any value. The range in which they can vary is given by the physical engine mounts.

Assumed allowed range for design parameters: $500 < Ceijk < 50000$

The initial guess are the properties of the conventional mounting system.

Initial guess: $Ce1yy = 1670\ ;\ Ce2zz = Ce3zz = 2770$

Optimal values for the design variables for different sets of excitations shall be found.

5.3.2 Turning on the engine

Excitations: Dynamic excitations 3 (chapter 5.1.2.1.), no kinematic excitations (the vehicle is standing still)

Simulation time: 3 s

The objective and constraints are calculated for the whole simulation time: 0 s to 3 s

Results

Results of the optimization process:

$\hat{C}e1yy = 12705$; $\hat{C}e2zz = \hat{C}e3zz = 50000$

$\hat{g} = 0.2077$

The standard values:

$Ce1yy_0 = 1670$; $Ce2zz_0 = Ce3zz_0 = 2770$

$g_0 = 0.4867$

The improvement due to the optimization can be expressed as:

$$1 - \frac{\hat{g}}{g_0} = 0.5732$$

That means the optimized mounting system produces for this special operating condition 57.32% less vibrations, compared to the initial guess.

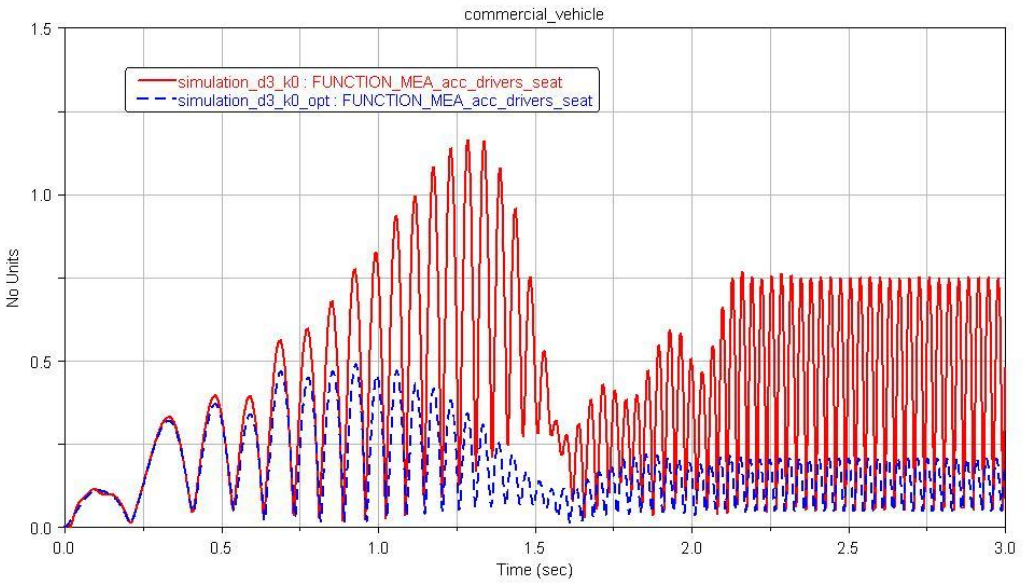

Figure 18: Magnitude of the acceleration of the driver's seat. Optimal (- - -); Initial guess (—)

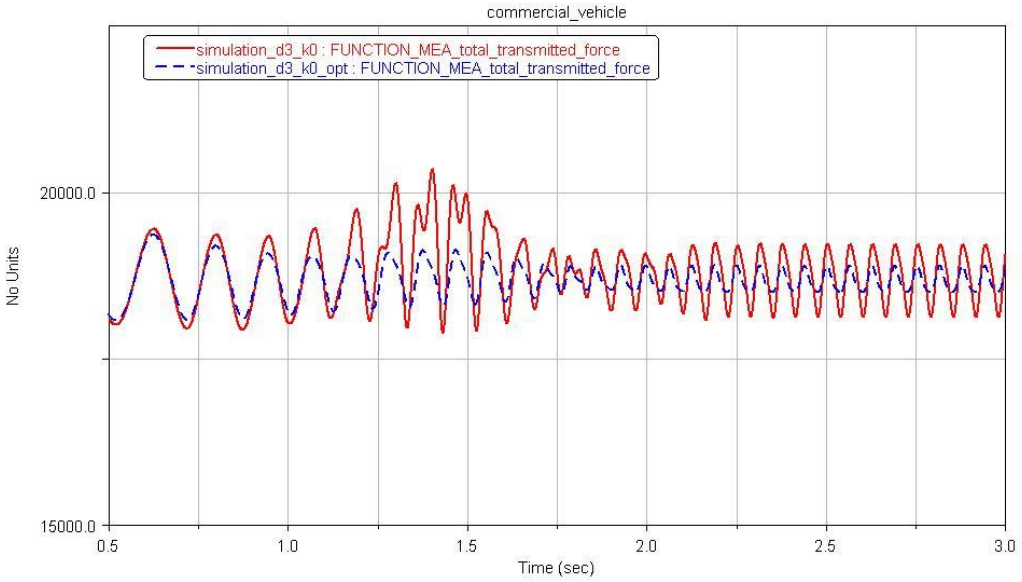

Figure 19: Total transmitted force. Optimal (- - -); Initial guess (—)

A considerable decrease of both the accelerations of the chassis and the transmitted force due to the optimized damping parameters is clearly visible.

5.3.3 Driving on good road with high engine speed

Excitations: Kinematic excitations 2, Dynamic excitations 1

Simulation time: 1.5 s

The objective is calculated from the end of the transient oscillations to the beginning of the kinematic excitations: 0.5 s to 0.85 s

The constraints are calculated from the end of the transient oscillations to the end of the simulation: 0.5 s to 1.5 s

Results

Results of the optimization process:

$\hat{\mathrm{C}}\mathrm{e1yy} = 5440.5$; $\hat{\mathrm{C}}\mathrm{e2zz} = \hat{\mathrm{C}}\mathrm{e3zz} = 31793$

$\hat{\mathrm{g}} = 0.01355$

The standard values:

$\mathrm{Ce1yy}_0 = 1670$; $\mathrm{Ce2zz}_0 = \mathrm{Ce3zz}_0 = 2770$

$\mathrm{g}_0 = 0.04344$

The improvement due to the optimization can be expressed as:

$$1 - \frac{\hat{\mathrm{g}}}{\mathrm{g}_0} = 0.6881$$

That means the optimized mounting system produces for this special operating condition 68.81% less vibrations, compared to the initial guess.

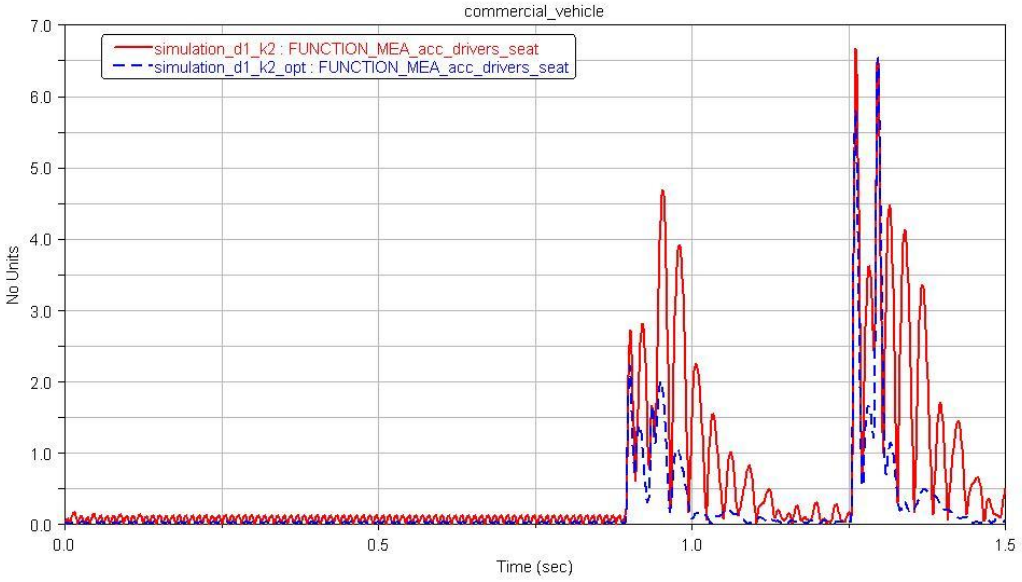

Figure 20: Magnitude of the acceleration of the driver's seat. Optimal (- - -); Initial guess (—)

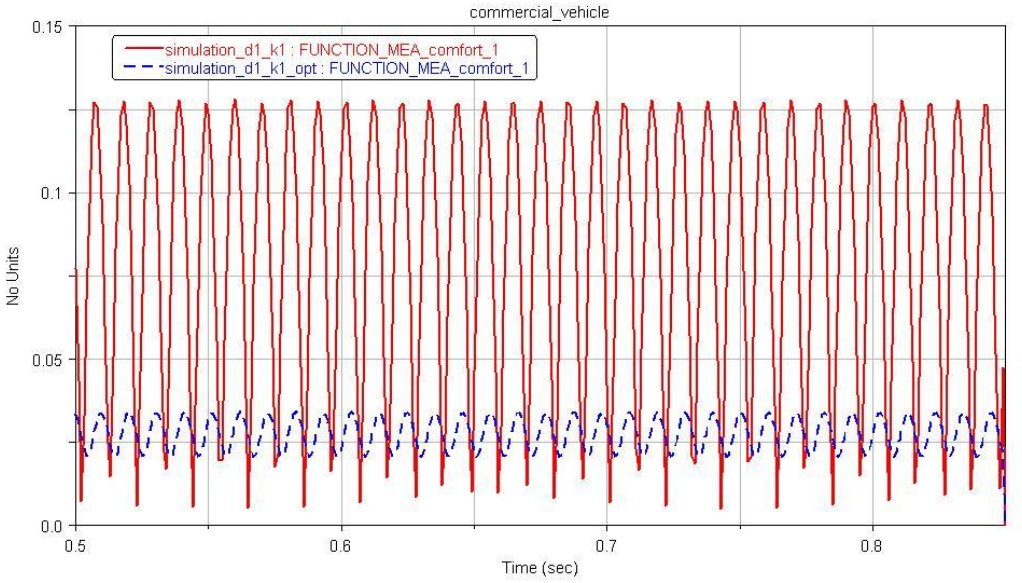

Figure 21: Magnitude of the acceleration of the driver's seat. Optimal (- - -); Initial guess (—)

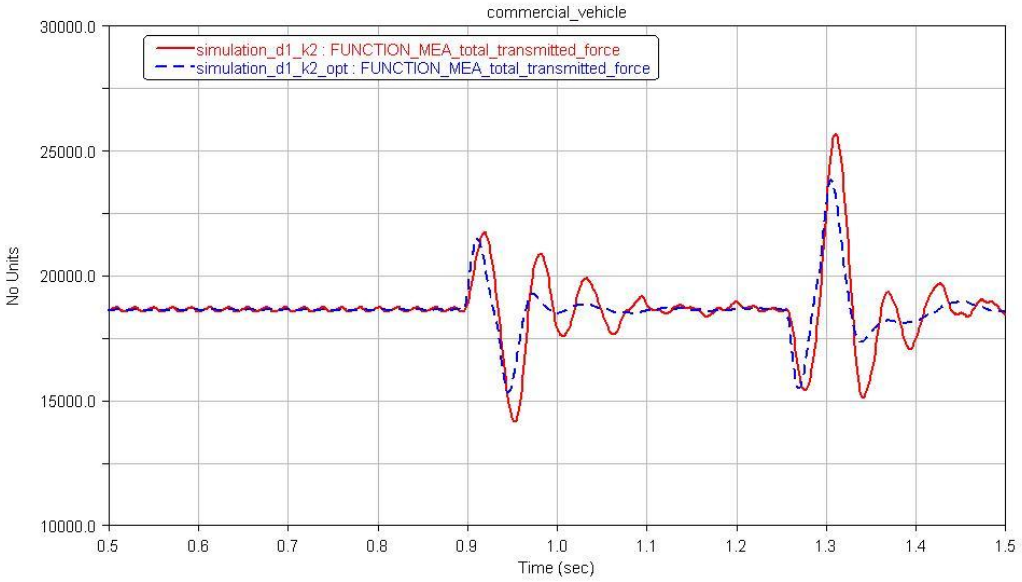

Figure 22: Total transmitted force. Optimal (- - -); Initial guess (—)

As long as no kinematic excitations are affecting the model both the accelerations of the chassis and the transmitted force are reduced clearly. But the kinematic excitations cause accelerations and transmitted forces which are indeed smaller in average but their maximum is almost not affected by the optimized damping.

5.3.4 Driving on bad road with high engine speed

Excitations: Kinematic excitations 1 (chapter 5.1.2.2.), Dynamic excitations 1 (chapter 5.1.2.1.)

The objective is calculated from the end of the transient oscillations to the beginning of the kinematic excitations: 0.5 s to 0.85 s

The constraints are calculated from the end of the transient oscillations to the end of the simulation: 0.5 s to 1.5 s

Results

Results of the optimization process:

$\hat{\mathrm{C}}\mathrm{e1yy} = 5440.5\ ;\ \hat{\mathrm{C}}\mathrm{e2zz} = \hat{\mathrm{C}}\mathrm{e3zz} = 31793$

$\hat{\mathrm{g}} = 0.01355$

The standard values:

$\mathrm{Ce1yy}_0 = 1670\ ;\ \mathrm{Ce2zz}_0 = \mathrm{Ce3zz}_0 = 2770$

$\mathrm{g}_0 = 0.04344$

The improvement due to the optimization can be expressed as:

$$1 - \frac{\hat{\mathrm{g}}}{\mathrm{g}_0} = 0.6881$$

That means the optimized mounting system produces for this special operating condition 68.81% less vibrations, compared to the initial guess.

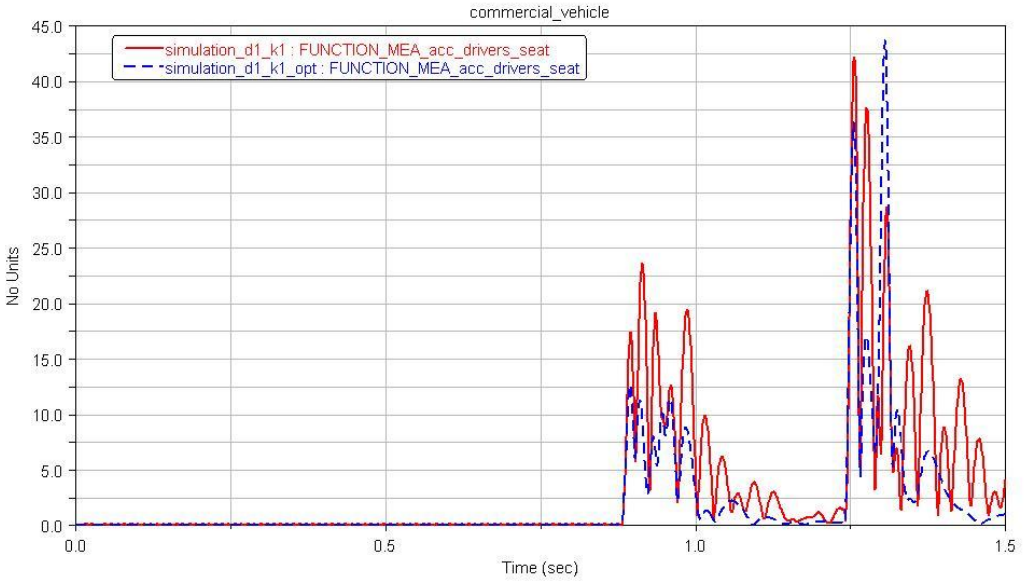

Figure 23: Magnitude of the acceleration of the driver's seat. Optimal (- - -); Initial guess (—)

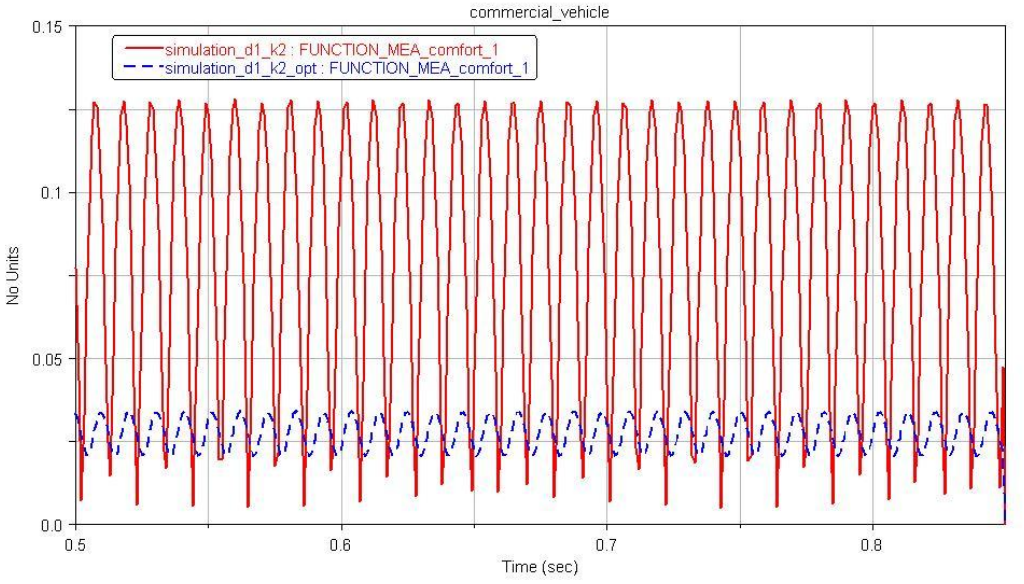

Figure 24: Magnitude of the acceleration of the driver's seat. Optimal (- - -); Initial guess (—)

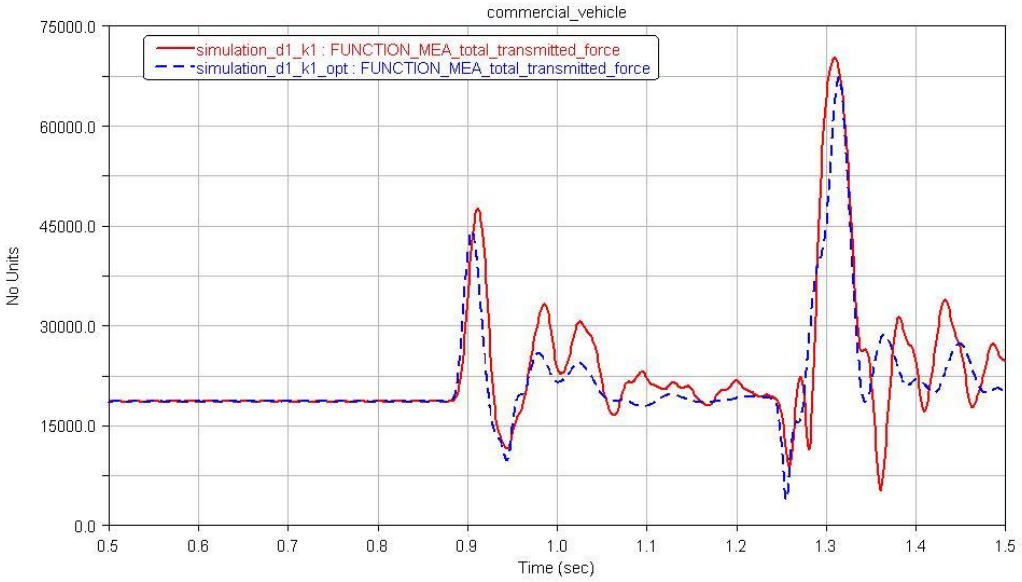

Figure 25: Total transmitted force. Optimal (- - -); Initial guess (—)

Until the kinematic excitations start the simulation is exactly the same as the one above. Because the objective is only calculated in this section and the constraints are not violated in the third section the optimal setting for the mount damping is also the same as before. But since the kinematic excitations are stronger as before the maximum of the magnitude of accelerations of the driver's seat is even higher but still fulfilling the constraint.

5.3.5 Driving on good road with low engine speed

Excitations: Kinematic excitations 2 (chapter 5.1.2.2.), Dynamic excitations 2 (chapter 5.1.2.1.)

The objective is calculated from the end of the transient oscillations to the beginning of the kinematic excitations: 0.5 s to 0.85 s

The constraints are calculated from the end of the transient oscillations to the end of the simulation: 0.5 s to 1.5 s

Results

Results of the optimization process:

$\hat{\mathrm{C}}\mathrm{e1yy} = 50000\ ;\ \hat{\mathrm{C}}\mathrm{e2zz} = \hat{\mathrm{C}}\mathrm{e3zz} = 50000$

$\hat{\mathrm{g}} = 0.04131$

The standard values:

$\mathrm{Ce1yy}_0 = 1670\ ;\ \mathrm{Ce2zz}_0 = \mathrm{Ce3zz}_0 = 2770$

$\mathrm{g}_0 = 0.2060$

The improvement due to the optimization can be expressed as:

$$1 - \frac{\hat{g}}{g_0} = 0.7995$$

That means the optimized mounting system produces for this special operating condition 79.95% less vibrations, compared to the initial guess.

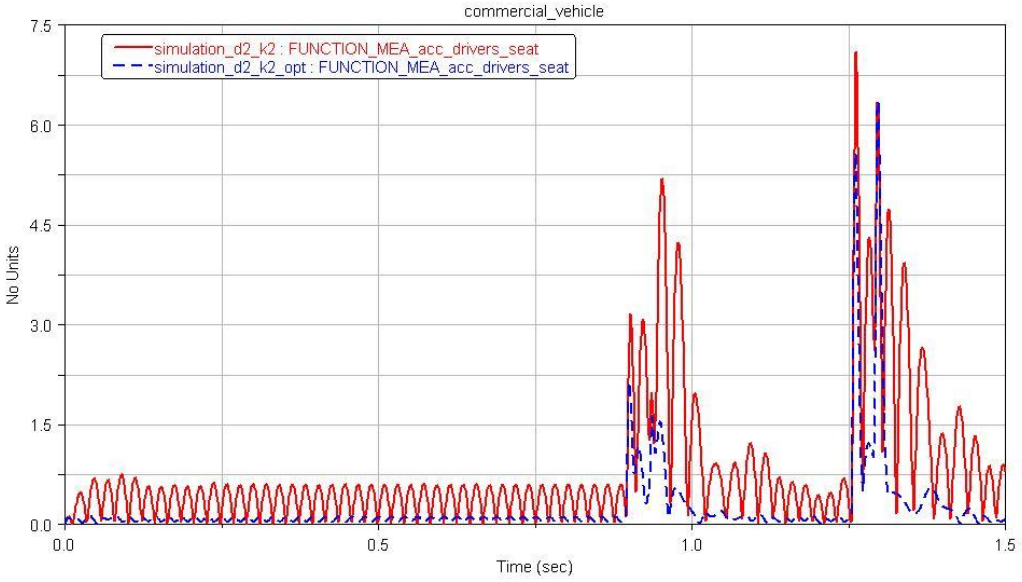

Figure 26: Magnitude of the acceleration of the driver's seat. Optimal (- - -); Initial guess (—)

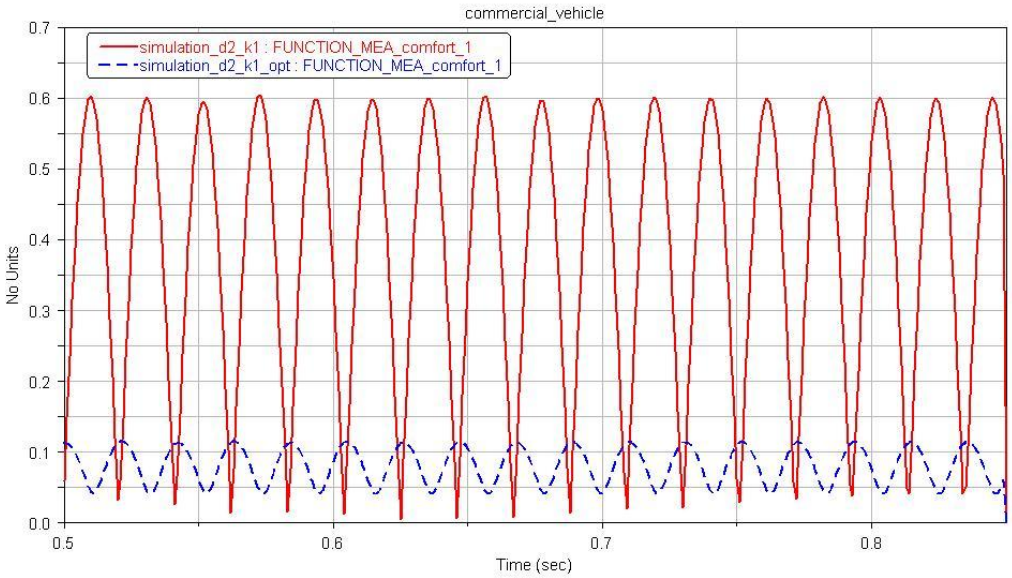

Figure 27: Magnitude of the acceleration of the driver's seat. Optimal (- - -); Initial guess (—)

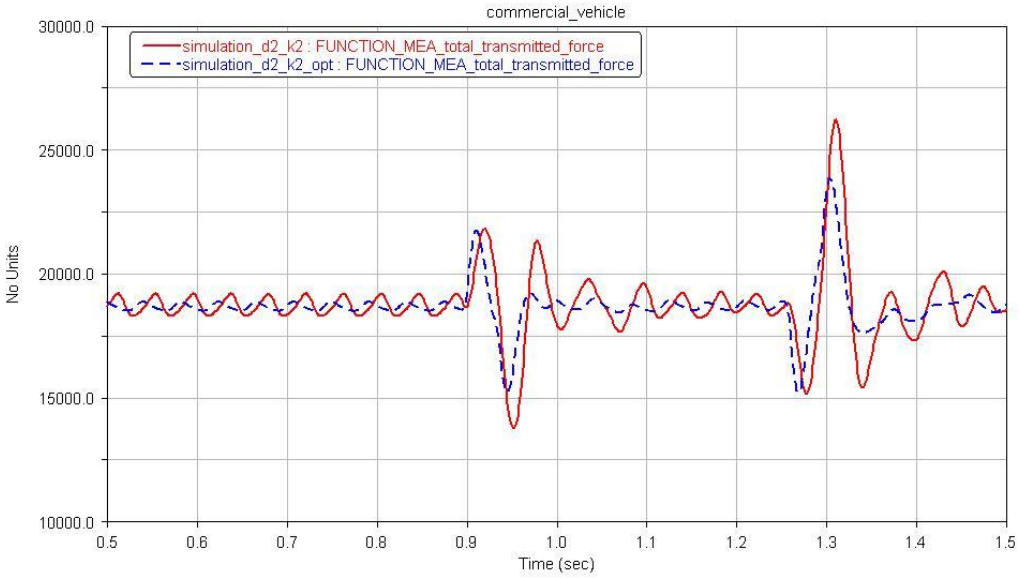

Figure 28: Total transmitted force. Optimal (- - -); Initial guess (—)

The results look quite similar to those from good road with high engine speed. The achieved reduction of chassis vibrations is even bigger. But of course since the amplitude of the dynamic excitations is higher, both the accelerations of the chassis and the transmitted forces are bigger.

5.3.6 Driving on bad road with low engine speed

Excitations: Kinematic excitations 1 (chapter 5.1.2.2.), Dynamic excitations 2 (chapter 5.1.2.1.)

The objective is calculated from the end of the transient oscillations to the beginning of the kinematic excitations: 0.5 s to 0.85 s

The constraints are calculated from the end of the transient oscillations to the end of the simulation: 0.5 s to 1.5 s

Results

Results of the optimization process:

$\hat{\mathrm{C}}\mathrm{e1yy} = 50000\ ;\ \hat{\mathrm{C}}\mathrm{e2zz} = \hat{\mathrm{C}}\mathrm{e3zz} = 50000$

$\hat{\mathrm{g}} = 0.04131$

The standard values:

$\mathrm{Ce1yy}_0 = 1670\ ;\ \mathrm{Ce2zz}_0 = \mathrm{Ce3zz}_0 = 2770$

$\mathrm{g}_0 = 0.2060$

The improvement due to the optimization can be expressed as:

$$1 - \frac{\hat{\mathrm{g}}}{\mathrm{g}_0} = 0.7995$$

That means the optimized mounting system produces for this special operating condition 79.95% less vibrations, compared to the initial guess.

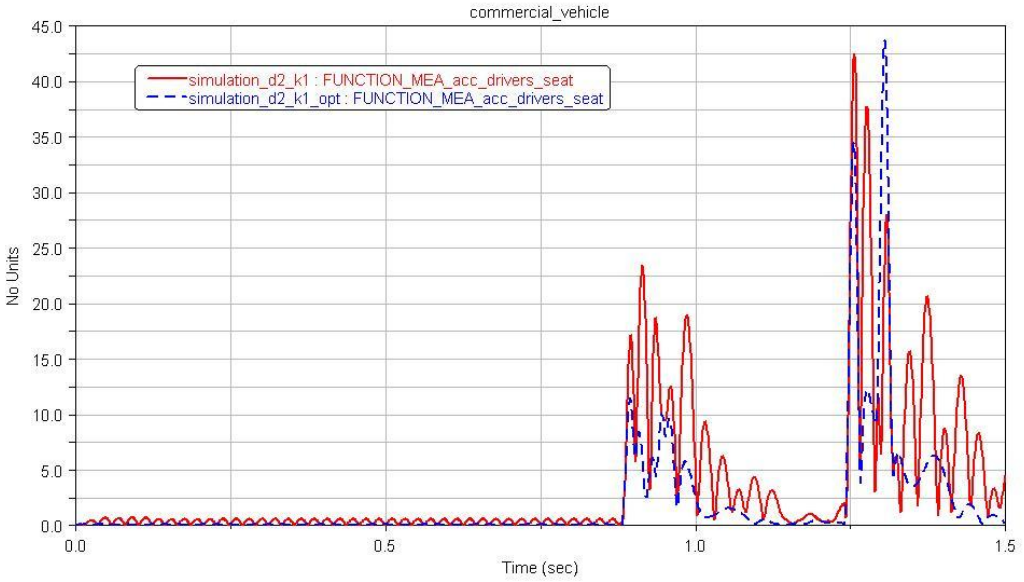

Figure 29: Magnitude of the acceleration of the driver's seat. Optimal (- - -); Initial guess (—)

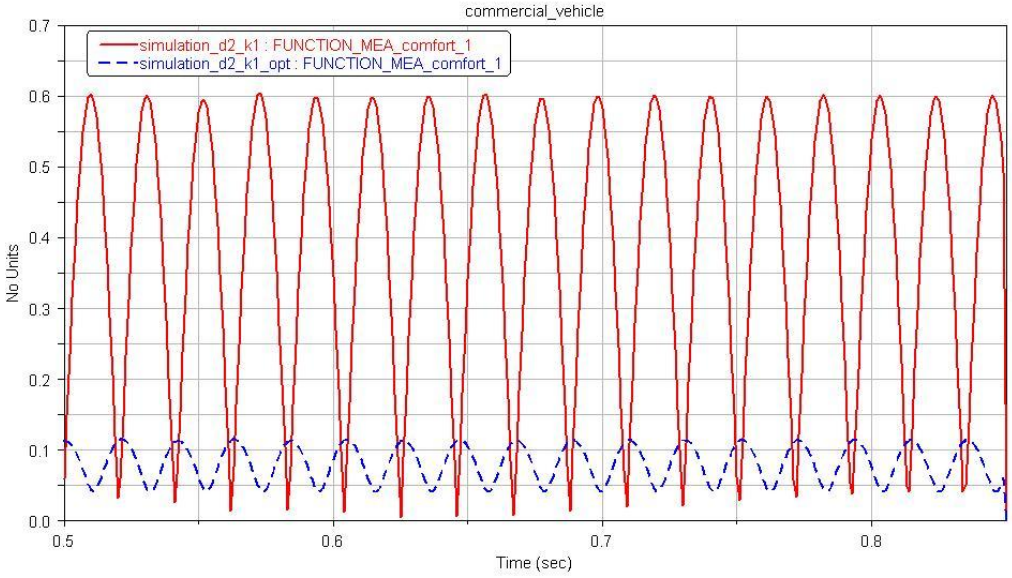

Figure 30: Magnitude of the acceleration of the driver's seat. Optimal (- - -); Initial guess (—)

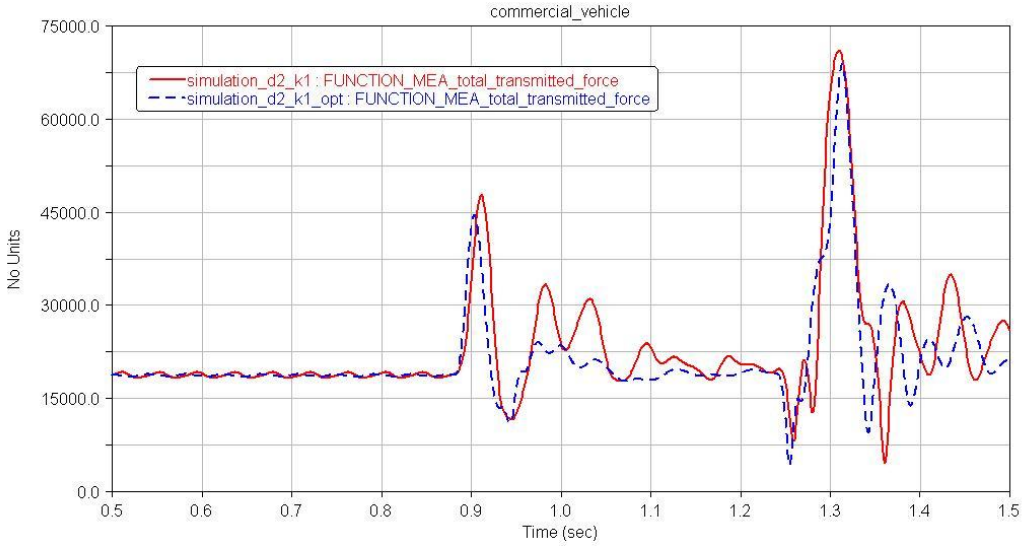

Figure 31: Total transmitted force. Optimal (- - -); Initial guess (—)

Again the simulation is exactly the same as the one above until the kinematic excitations start. And also the optimal setting for the mount damping is also the same as before. But since the kinematic excitations are stronger as before the maximum of the magnitude of accelerations of the driver's seat is even higher.

5.3.7 Conclusion of optimization

The few optimizations presented above exemplify that great improvements of the vibrations caused by the engine are reachable by dint of adaptive engine mounts. The optima seem to be independent of the kinematic excitations. That means an easy way to implement an adaptive mounting system is one consisting of mounts with tunable damping open loop controlled by the operating state of the engine. But the improvement of comfort the driver will notice will be not very big on a bad road, because there are the vibrations of the chassis mainly dominated by the kinematic excitations.

In the same way some of the damping parameters were optimized here, other characteristics of the engine mounting system can be improved, for example the stiffness, orientation or location of the mounts.

6 Conclusion and recommendations for future research

This paper presents the mechanical, mathematical and computational models of a four wheel ground vehicle with three point engine mounting system. Such a vehicle is reduced to a rigid body system with 13 degrees of freedom. Consisting of chassis, engine, four unsprung wheel masses, linear springs and dampers for the tires and suspension and engine mounts with three dimensional stiffness and damping. The mathematical model consists of a set of differential equations describing the dynamics of the system. The computational model is created with MSC Adams View. It provides the possibility to analyse the vibration dynamics of any suchlike vehicle under dynamic and kinematic excitations. Dynamic excitations are the forces and torques caused by the working process of the engine and kinematic excitations are motions of the wheel bases enforced by the uneven surface of the road. Both excitations can be described by any time dependent function. Furthermore Adams enables to run design parameter optimizations. Several simulations with special input to verify the model were run.

Examples for both abilities are presented in this thesis. The vibration dynamics of a commercial vehicle under different operating conditions are analysed. And the damping of the mounts is optimized for different sets of kinematic and dynamic excitations. Since the purpose of this study is the improvement of the comfort, the objective for those optimizations is the vibration of the chassis.

One of the results of those simulations is that, consistent to the daily experience, as long as the road is not very smooth it is the main source of vibrations in a vehicle. That means the improvement of comfort achievable with advanced engine mounting systems is limited. But nevertheless the vibrations caused by the dynamic excitations can be reduced seriously with optimized mount damping. From this can follow a setup of an adaptive engine mounting system.

The next steps to continue this work could be:

- Implementation of a more advanced mount model. The applied linear spring-damper in parallel model is fairly simplified.
- More advanced models for the excitations. A more realistic surface of the road would allow better predictions about the achievable improvements.
- Taking into account the elasticity of the chassis. The influence of this should not be underestimated since resonance phenomena can occur if the excitations cross one of the chassis natural frequencies.
- Adoption of time-dependent mount properties. Especially as Fourier series with multiple frequencies of the engine speed could be auspicious.
- Implementation of controls for some of the mount properties.

7 References

[1] Seung-Bok Choi, Hyun-Jeong Song, 2002, "Vibration Control of a Passenger Vehicle Utilizing a Semi-Active ER Engine Mount", Vehicle System Dynamics, 2002, Vol. 37, No. 3, pp. 193-216

[2] Cihan Bayram, Mehmet Hakan Ugun, 2008, "Towards Modelling of Engine Vibration Dynamics of Commercial Vehicle", Master of automotive engineering, Chalmers University, Göteborg, Sweden

[3] Claes Olsson, 2006, "Active automotive engine vibration isolation using feedback control", Journal of Sound and Vibration 294 (2006) pp. 162–176

[4] Hoda Yarmohamadi, Viktor Berbyuk, 2008, "Vibration dynamics of a commercial vehicle engine suspended on adaptronic mounting system", The 9th International Conference on Motion and Vibration Control, September 15-18, 2008, Technische Universität München, Munich, Germany, s. 1-10

[5] Chiharu Togashi, Ken Ichiryu, 2003, "Study on Hydraulic Active Engine Mount", Noise & Vibration Conference and Exhibition, Traverse City, Michigan, May 5-8, 2003

[6] Yunhe Yu, Saravanan M. Peelamedu, Nagi G. Naganathan, Rao V. Dukkipati, 2001, "Automotive Vehicle Engine Mounting Systems: A Survey", Journal of Dynamic Systems, Measurement, and Control, Vol. 123, June 2001, pp.186-194

[7] G. Kim, R. Singh, 1993, "A Study of Passive and Adaptive Hydraulic Engine Mount Systems with Emphasis on Non-Linear Characteristics", Journal of Sound and Vibration" 179 (1995) pp. 427–453

[8] Y-W Lee, C-W Lee, 2002, " Dynamic analysis and control of an active engine mount system", Proc Instn Mech Engrs Vol 216 Part D: J Automobile Engineering

[9] Seung-Bok Choi, Jung Woo Sohn, Young-Min Han, Jung-Wook Kim, 2008, "Dynamic Characteristics of Three-axis Active Mount Featuring Piezoelectric Actuators", Journal of Intelligent Material Systems and Structures, Vol. 19, September 2008

[10] A. R. Ohadi, G. Maghsoodi, 2007, "Simulation of Engine Vibration on Nonlinear Hydraulic Engine Mounts", Journal of Vibration and Acoustics Vol. 129, August 2007

8 Appendix

8.1 Detailed description of the Adams model

Gravity is in the negative z-direction and the front of the vehicle is in the positive x-direction. The used unit system is MKS.

The following description of the front left wheel unit is exemplary for the other wheels.

The four wheels are called:

fl or 1 for the front left wheel

fr or 2 for the front right wheel

rr or 3 for the rear right wheel

rl or 4 for the rear left wheel

A point called POINT_wheelbase_fl is connected to the ground at the position ((DV_wheel_f_x), (DV_wheel_l_y), 0).

A part called PART_ wheelbase_fl is connected to the ground by a primitive orientation joint (JOINT_wheelbase_fl) which allows motion in the x-, y- and z-direction. The motions in x- and y-direction are free the one in z-direction is controlled by the kinematic excitation. The general motion of the joint is named general_motion_kin_exc_fl. This body has the mass 0.001. Its CM is at given by: (LOC_RELATIVE_TO({0, 0, 0}, POINT_wheelbase_fl)).

A part called PART_unsp_wm_fl with the mass DV_m_us_f representing the unsprung wheel mass is connected to the previous body by a translational join (JOINT_unsp_wm_fl) which allows motion in the z direction. Its CM is given by (LOC_RELATIVE_TO({0, 0, 0}, POINT_unsp_wm_fl)).

A spring called SPRING_tire_fl with the stiffness DV_ku_f and the damping DV_cu_f is attached between the CM's of PART_wheelbase_fl and PART_unsp_wm_fl.

The tire and suspension springs are preloaded so that the positions of the parts at the static equilibrium are the mentioned (chapter 8.4.).

A point called POINT_cm_chassis is connected to the ground at the position (0,0,1.5).

There is a part called PART_chassis with the mass DV_mc and the inertia Ixx= (DV_Icxx) Iyy= (DV_Icyy) and Izz= (DV_Icyy - DV_Icxx) (Off Diagonal Terms). It has the Diag Corner Coords ((DV_wheel_f_x - DV_wheel_r_x),(DV_wheel_l_y - DV_wheel_r_y),1.0). Its corner marker is at the position (LOC_RELATIVE_TO({DV_wheel_r_x, DV_wheel_r_y, -0.5},POINT_cm_chassis)). It's CM is at the position (LOC_RELATIVE_TO({0, 0, 0}, POINT_cm_chassis)).It is connected to the ground by a primitive inline joint which is called JOINT_chassis and allows displacement in z-direction and rotation around the x- and y'- axis the rotation around the z''-axis is fixed.

A spring called SPRING_suspension_fl with the stiffness DV_ks_f and the damping DV_cs_f is attached between the CMs' of unsp_wm_fl and Marker at the corner of PART_chassis. (For preload see chapter 8.4.)

A primitive inline joint called JOINT_suspension_fl connects PART_chassis with PART_unsp_wm_fl. It is a 2 Bodies - 2 Locations joint. Its directions are the z-directions on a marker on PART_chassis and PART_unsp_wm_fl.

That means there are now 4 d.o.f.s for the unsp_wm_xx in z-direction, 1 d.o.f. for the motion of the chassis in z-direction and 2 d.o.f.s for the rotation of the chassis around the x- and y-axis.

A point called POINT_cm_engine is connected to PART_chassis at the position ((DV_ex), (DV_ey), (DV_ez)).

A part called PART_engine with the mass DV_me and the inertia tensor (DV_Iexx, DV_Iexy, DV_Iexz, DV_Ieyy, DV_Ieyz; DV_Iezz) has its CM at the position (LOC_RELATIVE_TO({0, 0, 0}, POINT_cm_engine)). It has the Diag Corner Coords ((DV_rc1x - DV_rc2x),(DV_rc1y - DV_rc3y),0.5). It's corner marker is at the position ((DV_rc2x),(DV_rc3y),(1.45 + DV_rc3z)).

The following description of the mount1 is exemplary for all three mounts.

A point called POINT_r1 is connected to PART_chassis at the position ((DV_rc1x), (DV_rc1y), (DV_rc1z+1.5)).

A marker called MARKER_re1 connected to PART_engine and a marker called MARKER_rc1 connected to PART_chassis are both located at (LOC_RELATIVE_TO({0, 0, 0}, POINT_r1)).

Between each of those pairs of markers is a six component force attached, acting on the engine reacting on the chassis with its components give in chassis fixed coordinates. Those forces behave like three dimensional springs and dampers with a constant preload in z-direction (chapter 8.5.). The exact Adams code describing those forces is given in the chapter 8.6. The reference marker for the mount force has also the orientation ((DV_a11),(DV_a12),(DV_a13)).

That means there are another 6 d.o.f.s for the motion of the engine.

A six component general force (GFORCE_dyn_exc) affects the engines CM (acting on the engine, reacting on the ground, reference marker PART_engine.cm). Those six components are given by the dynamic excitations.

A marker is called MARKER_driver connected to PART_chassis located at (1.8, 0.8, 2.0).

8.2 Verification

The verification was done with parameters for a personal vehicle.

8.2.1 Standard parameter settings

wheel_f_x	x-position of the front wheels	1.4
wheel_r_x	x-position of the rear wheels	-1.4
wheel_r_y	y-position of the right wheels	-0.72
wheel_l_y	y-position of the left wheels	0.72
mc	mass of the chassis	868
me	mass of the engine	244
m_us_f	unsprung wheel mass front	29.5
m_us_r	unsprung wheel mass rear	27.5
ku_f	stiffness of the front tire	200000
ku_r	stiffness of the rear tire	200000
cu_f	damping of the front tire	0
cu_r	damping of the rear tire	0
ks_f	stiffness of the front suspension	20580
ks_r	stiffness of the rear suspension	19600
cs_f	damping of the front suspension	3200
cs_r	damping of the rear suspension	1700
Icxx	Moment of inertia of the chassis around the x-axis (roll)	235
Icyy	Moment of inertia of the chassis around the y-axis (pitch)	920
Iexx	Moment of inertia of the engine	30.7
Ieyy	Moment of inertia of the engine	37.25
Iezz	Moment of inertia of the engine	34.73
Iexy	Moment of inertia of the engine	-1.6
Iexz	Moment of inertia of the engine	9.08
Ieyz	Moment of inertia of the engine	-5.64
ex	x-position of the engine CM w.r.t. the CM of the chassis	0.8994
ey	y-position of the engine CM w.r.t. the CM of the chassis	-0.12765
ez	z-position of the engine CM w.r.t. the CM of the chassis	-0.0049
Ke1xx	translational stiffness on the 1st mount	66000
Ke1yy	translational stiffness on the 1st mount	66000
Ke1zz	translational stiffness on the 1st mount	225000

Ke2xx	translational stiffness on the 2nd mount	66000
Ke2yy	translational stiffness on the 2nd mount	66000
Ke2zz	translational stiffness on the 2nd mount	225000
Ke3xx	translational stiffness on the 3ed mount	66000
Ke3yy	translational stiffness on the 3ed mount	66000
Ke3zz	translational stiffness on the 3ed mount	225000
Ce1xx	translational damping on the 1st mount	20
Ce1yy	translational damping on the 1st mount	20
Ce1zz	translational damping on the 1st mount	98
Ce2xx	translational damping on the 2nd mount	20
Ce2yy	translational damping on the 2nd mount	20
Ce2zz	translational damping on the 2nd mount	98
Ce3xx	translational damping on the 3ed mount	20
Ce3yy	translational damping on the 3ed mount	20
Ce3zz	translational damping on the 3ed mount	98
rc1x	x-position of mount 1 w.r.t. the cm of the chassis	1.11
rc2x	x-position of mount 2 w.r.t. the cm of the chassis	0.6688
rc3x	x-position of mount 3 w.r.t. the cm of the chassis	0.7754
rc1y	y-position of mount 1 w.r.t. the cm of the chassis	0.0839
rc2y	y-position of mount 2 w.r.t. the cm of the chassis	0.0839
rc3y	y-position of mount 3 w.r.t. the cm of the chassis	-0.6092
rc1z	z-position of mount 1 w.r.t. the cm of the chassis	-0.151
rc2z	z-position of mount 2 w.r.t. the cm of the chassis	-0.151
rc3z	z-position of mount 3 w.r.t. the cm of the chassis	-0.2549

8.2.2 Verification experiments

8.2.2.1 Experiment 1

Mass of the engine equals nearly zero. Engine is fixed at the chassis. No dynamic excitations. All kinematic excitations are sinusoidal with equal amplitudes, frequency and phase. That means the model behaves like a two mass oscillator. The magnitude of the systems response (motion of the chassis and unsprung wheel masses in z-direction) is measured for excitation with different frequencies. The response is expected to be maximal for excitations with the two natural frequencies. Those measured natural frequencies can be compared with the analytically calculated.

Special parameters

me	mass of the engine	0.001
m_us_f	unsprung wheel mass front	29.5
m_us_r	unsprung wheel mass rear	29.5
ks_f	stiffness of the front suspension	20580
cs_f	damping of the front suspension	500
ks_r	stiffness of the rear suspension	20580
cs_r	damping of the rear suspension	500

Special constraints

The engine is connected to the chassis by a fixed joint. The roll and pitch d.o.f.s of the chassis are fixed.

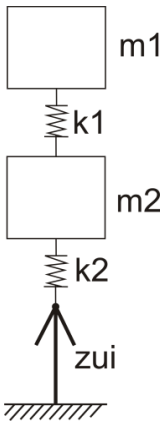

Excitations

Dynamic excitations:

$$F_{dx} = F_{dy} = F_{dz} = M_{dx} = M_{dy} = M_{dz} = 0$$

Kinematic excitations:

$$z_{u1} = z_{u2} = z_{u3} = z_{u4} = 0.01\sin(\omega t)$$

Analytical prediction

The system behaves like a two mass oscillator. The two natural frequencies can be calculated as follows.

$$\lambda^2 = -\frac{m_1(k_1+k_2)+m_2k_1}{2m_1m_2} \pm \sqrt{\left(\frac{m_1(k_1+k_2)+m_2k_1}{2m_1m_2}\right)^2 - \frac{k_1k_2}{m_1m_2}}$$

$$\lambda = \pm i\omega$$

$$m_1 = m_c \;;\; m_2 = \sum m_{ui} \;;\; k_1 = \sum k_{si} \;;\; k_2 = \sum k_{ui}$$

$$\Rightarrow \omega_1 = 9.2676$$

$$\Rightarrow \omega_2 = 86.5231$$

Results

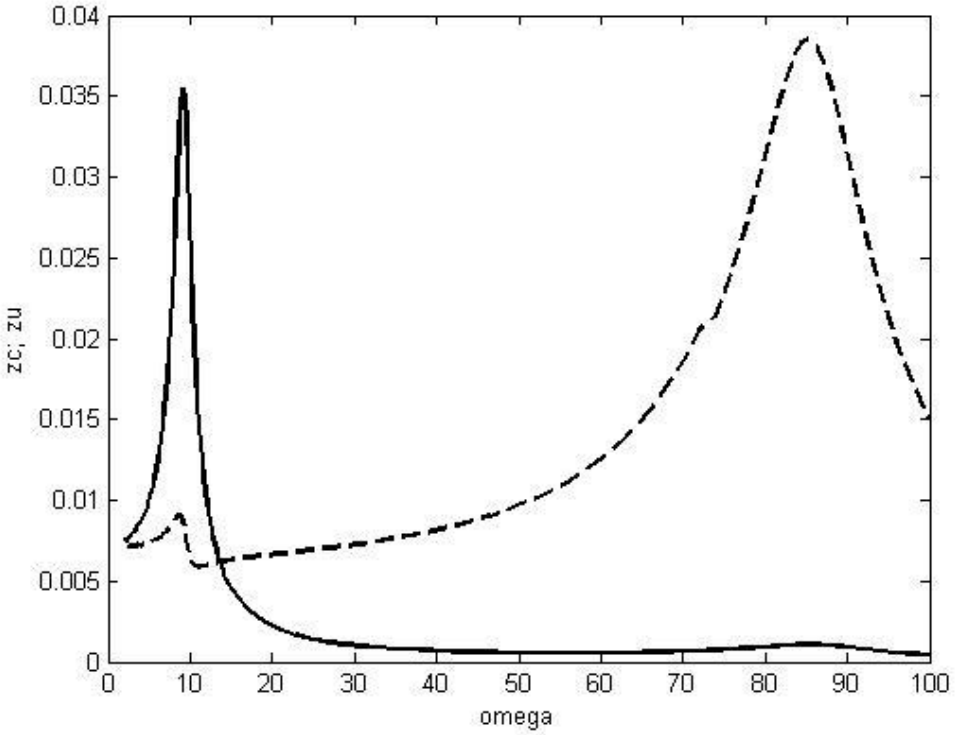

Figure 32: System response for kinematic excitations with different frequencies (zc: ── ; zu: - - -)

Discussion

The response of the system has clearly visible maxima for excitations which fit pretty good to the calculated natural frequencies.

Calculated: $\omega_1 = 9.2676$ Measured: $\omega_1 = 8.801$

$\omega_2 = 86.5231$ $\omega_2 = 85.104$

The differences between the expected and the measured natural frequencies are caused by the damping. Damping reduces the natural frequencies marginal. If the damping gets to high, the peaks in the systems response at the natural frequencies disappear.

8.2.2.2 Experiment 2

The same as experiment 1 but there is a second sinusoidal kinematic excitation superposing the first one but with higher frequency and about π out of phase between the right and the left side. Now the chassis rotates with the frequency of the second excitation around the x-axis. If the inertia about the x-axis is changed to bigger values, these rotations are expected to get smaller amplitudes.

Special parameters

me	mass of the engine	0.001
Icxx	Moment of inertia of the chassis about the x-axis (roll)	parameter
Icyy	Moment of inertia of the chassis about the y-axis (pitch)	parameter

Special constraints

The engine is connected to the chassis by a fixed joint.

Excitations

Dynamic excitations:

$F_{dx} = F_{dy} = F_{dz} = M_{dx} = M_{dy} = M_{dz} = 0$

Kinematic excitations:

$z_{u1} = z_{u4} = 0.2\sin(\omega_1 t) + 0.1\cos(\omega_2 t)$

$z_{u2} = z_{u3} = 0.2\sin(\omega_1 t) + 0.1\sin(\omega_2 t)$

$\omega_1 = 10$

$\omega_2 = 23$

Analytical prediction

The inertia but not the mass of the chassis is modified to different values. For bigger values the amplitude of the rotation of the chassis around the x-axis decreases. For smaller values the amplitude increases

Results

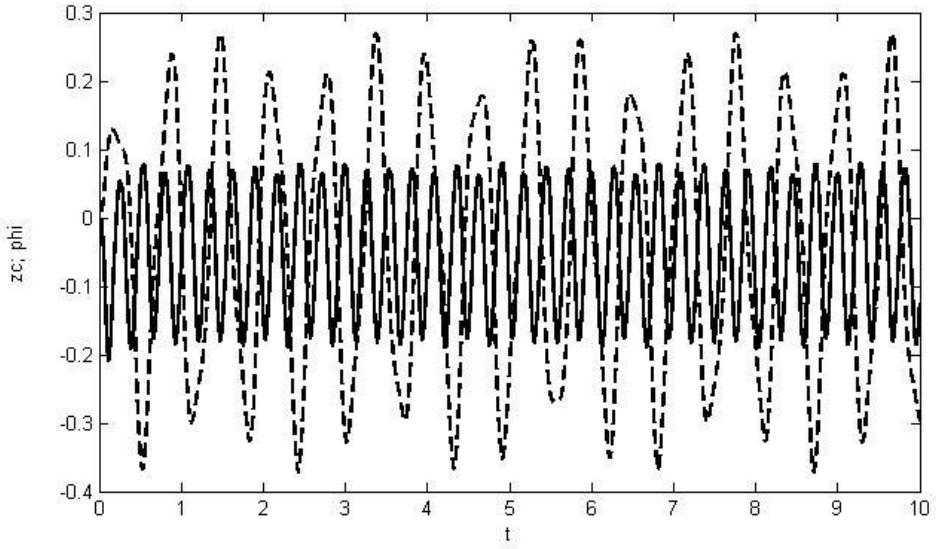

Figure 33: $I_{cxx} = 2.35$; $I_{cyy} = 9.2$
(phi: ── ; zc: - - -)

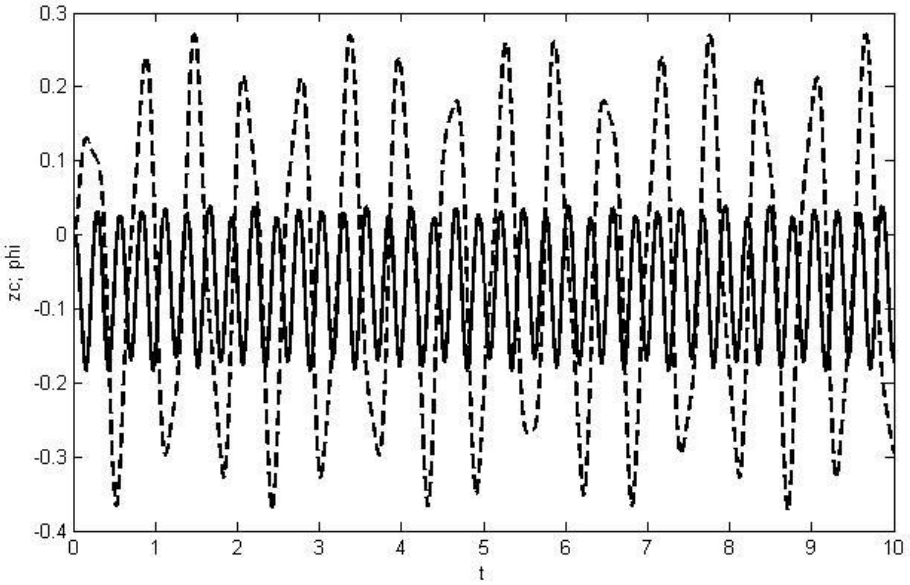

Figure 34: $I_{cxx} = 235$; $I_{cyy} = 920$
(phi: ── ; zc: - - -)

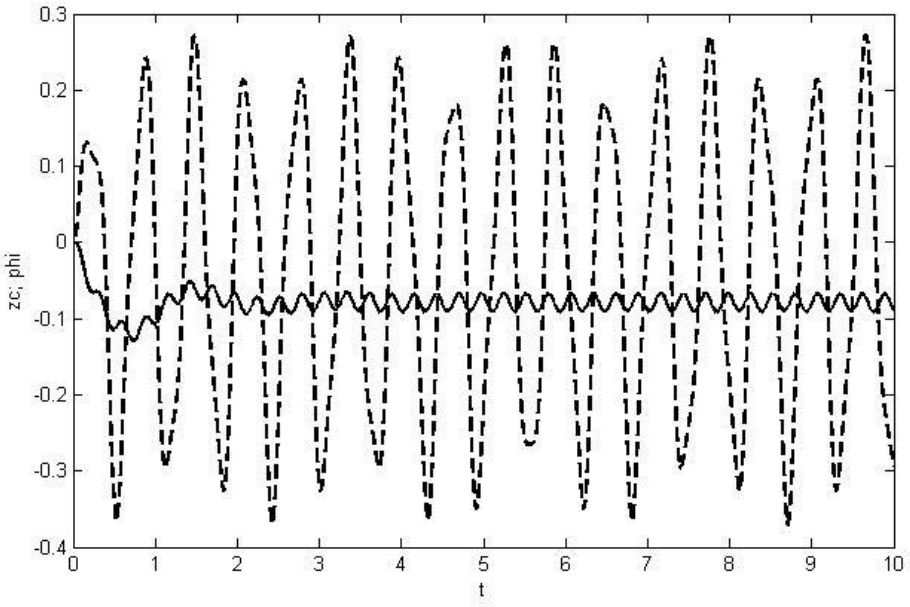

Figure 35: $I_{cxx} = 2350$; $I_{cyy} = 9200$
(phi: ── ; zc: - - -)

Discussion

It is clearly visible that the amplitude of the rotation around the x-axis (phi) decreases with increasing inertia. The motion along the z-axis (zc) is not affected by changes of the inertia as long as the mass is constant.

8.2.2.3 Experiment 3

The chassis is fixed to the ground and constant forces are applied on the engine. Each time one in a single direction. Now the static displacement can be compared with the one which was calculated by using the stiffness of the mounts. The sum of the transmitted forces, the static excitation force and the weight of the engine has to equal zero.

Special parameters

All parameters have standard values.

Special constraints

The chassis is fixed to the ground.

Excitations

Dynamic excitations:

$M_{dx} = M_{dy} = M_{dz} = 0$

I. $F_{dx} = 200\ ;\ F_{dy} = 0\ ;\ F_{dz} = 0$

II. $F_{dx} = 0\ ;\ F_{dy} = 200\ ;\ F_{dz} = 0$

III. $F_{dx} = 0\ ;\ F_{dy} = 0\ ;\ F_{dz} = 200$

Kinematic excitations:

$z_{u1} = z_{u2} = z_{u3} = z_{u4} = 0$

Analytic prediction

The total stiffness of the mounting system are:

$K_x = 3 * 66000 = 198000$

$K_y = 3 * 66000 = 198000$

$K_z = 3 * 225000 = 675000$

$K_i = \frac{F_i}{e\_i} \Leftrightarrow e\_i = \frac{F_i}{K_i}$

I. $e\_x = \frac{200}{198000} = 1.010 * 10^{-3}$

II. $e\_y = \frac{200}{198000} = 1.010 * 10^{-3}$

III. $e\_z = \frac{200}{675000} = 2.96 * 10^{-4}$

Results

I. $e_x = 0.0013\ ;\ e_y = -5.17e-5\ ;\ e_z = -7.91e-7$

$\alpha = 2.88e-4\ ;\ \beta = 0.0017\ ;\ \gamma = 6.42e-5$

$Ft_{1x} = -69.66\ ;\ Ft_{1y} = -0.442\ ;\ Ft_{1z} = 1161\ ;$

$Ft_{2x} = -69.71\ ;\ Ft_{2y} = 1.43\ ;\ Ft_{2z} = 501.66\ ;$

$Ft_{3x} = -60.63\ ;\ Ft_{3y} = -1.00\ ;\ Ft_{2z} = 730.49\ ;$

$$\sum F_x = -69.66 - 69.71 - 60.63 = -200 = -F_{dx}$$

$$\sum F_y = -0.442 + 1.43 - 1 = -0.012 \approx 0$$

$$\sum F_z = 1161 + 501.66 + 730.49 = 2393.15 \approx 2392.8 = -m_e g$$

II. $e_x = -5.21e-5$; $e_y = 0.0011$; $e_z = 3.18e-7$;

$\alpha = -5.66e-4$; $\beta = -2.41e-4$; $\gamma = 3.03e-4$;

$Ft_{1x} = 5.20$; $Ft_{1y} = -73.14$; $Ft_{1z} = 1090$;

$Ft_{2x} = 5.19$; $Ft_{2y} = -64.30$; $Ft_{2z} = 627.64$;

$Ft_{3x} = -10.33$; $Ft_{3y} = -62.56$; $Ft_{2z} = 675.65$;

$$\sum F_x = 5.20 + 5.19 - 10.33 = 0.06 \approx 0$$

$$\sum F_y = -73.14 - 64.30 - 62.56 = -200 = -F_{dy}$$

$$\sum F_z = 1090 + 627.64 + 675.65 = 2393.29 \approx 2392.8 = -m_e g$$

III. $e_x = -7.90e-5$; $e_y = 5.4423e-7$; $e_z = 3.16e-4$;

$\alpha = -1.46e-5$; $\beta = -4.16e-4$; $\gamma = -4.70e-5$;

$Ft_{1x} = 0.262$; $Ft_{1y} = 0.768$; $Ft_{1z} = 984.10$;

$Ft_{2x} = 0.260$; $Ft_{2y} = -0.601$; $Ft_{2z} = 539.46$;

$Ft_{3x} = -0.439$; $Ft_{3y} = -0.170$; $Ft_{2z} = 669.26$;

$$\sum F_x = 0.262 + 0.260 - 0.439 = 0.083 \approx 0$$

$$\sum F_y = 0.768 - 0.601 - 0.170 = -0.003 \approx 0$$

$$\sum F_z = 984.10 + 539.46 + 669.26 = 2193.82 \approx 2392.8 - 200 = -m_e g - F_{dz}$$

Discussion

The displacements of the engine fit pretty well to the predictions. The differences are caused by the rotations which were not considered in the prediction and in variations in the measure. The sums of forces are almost zero. The differences are caused by measuring faults.

8.2.2.4 Experiment 4

Mass of the engine equals nearly zero. Engine is fixed at the chassis. No kinematic excitations. The dynamic excitation in z-direction is sinusoidal. That means the model behaves like a two mass oscillator. The magnitude of the systems response (motion of the chassis and unsprung wheel masses in z-direction) is measured for excitation with different frequencies. The response is expected to be maximal for excitations with the two natural frequencies. Those measured natural frequencies can be compared with the analytically calculated.

Special parameters

me	mass of the engine	0.001
m_us_f	unsprung wheel mass front	29.5
m_us_r	unsprung wheel mass rear	29.5
ks_f	stiffness of the front suspension	20580
cs_f	damping of the front suspension	500
ks_r	stiffness of the rear suspension	20580
cs_r	damping of the rear suspension	500

Special constraints

The engine is connected to the chassis by a fixed joint. The roll and pitch d.o.f.s of the chassis are fixed.

Excitations

Dynamic excitations:

$F_{dx} = F_{dy} = M_{dx} = M_{dy} = M_{dz} = 0$

$F_{dz} = 200\sin(\omega t)$

Kinematic excitations:

$z_{u1} = z_{u2} = z_{u3} = z_{u4} = 0$

Analytic prediction

The system behaves like a two mass oscillator. The two natural frequencies can be calculated as follows.

$$\lambda^2 = -\frac{m_1(k_1+k_2)+m_2k_1}{2m_1m_2} \pm \sqrt{\left(\frac{m_1(k_1+k_2)+m_2k_1}{2m_1m_2}\right)^2 - \frac{k_1k_2}{m_1m_2}}$$

$\lambda = \pm i\omega$

$m_1 = m_c \;;\; m_2 = \sum m_{ui} \;;\; k_1 = \sum k_{si} \;;\; k_2 = \sum k_{ui}$

$\Rightarrow \omega_1 = 9.2676$

$\Rightarrow \omega_2 = 86.5231$

Results

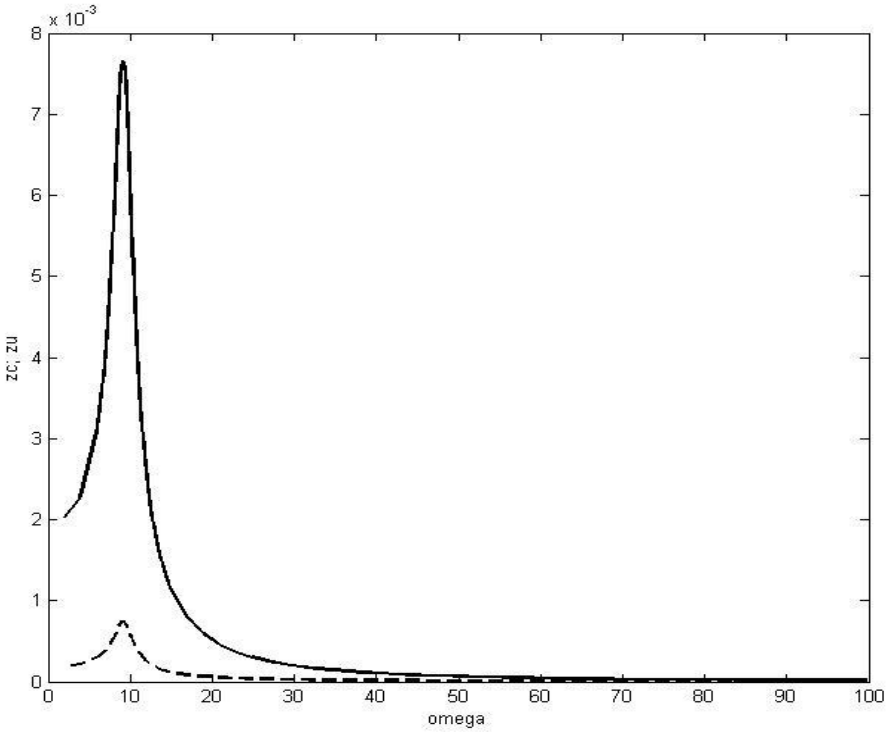

Figure 36: System response for dynamic excitations with different frequencies
(zc: ── ; zu: - - -)

Discussion

The first maximum of the systems response is clearly visible.

Calculated: $\omega_1 = 9.2676$ Measured: $\omega_1 = 9.16$

$\omega_2 = 86.5231$

The measured one is lower than the prediction but because damping lowers the natural frequencies this fits to the expectations.

The second maximum is not detectable. The reason for this is the large difference in the stiffness of the tire and suspension.

8.3 Parameters of the commercial vehicle

Adams variable	Mathematic symbol	Value	Description
DV_wheel_f_x	$(\tilde{r}_{s1})_x = (\tilde{r}_{s2})_x$	1.474 m	x-position of the front wheels w.r.t. the CM of the chassis
DV_wheel_r_x	$(\tilde{r}_{s3})_x = (\tilde{r}_{s4})_x$	-2.126 m	x-position of the rear wheels w.r.t. the CM of the chassis
DV_wheel_r_y	$(\tilde{r}_{s2})_y = (\tilde{r}_{s3})_y$	-1.245 m	y-position of the right wheels w.r.t. the CM of the chassis
DV_wheel_l_y	$(\tilde{r}_{s1})_y = (\tilde{r}_{s4})_y$	1.245 m	y-position of the left wheels w.r.t. the CM of the chassis
DV_m_us_f	$m_{u1} = m_{u2}$	80 kg	unsprung wheel mass front
DV_m_us_r	$m_{u3} = m_{u4}$	70 kg	unsprung wheel mass rear
DV_ku_f	$k_{u1} = k_{u2}$	2000000 N/m	stiffness of the front tire
DV_ku_r	$k_{u3} = k_{u4}$	2000000 N/m	stiffness of the rear tire
DV_cu_f	$c_{u1} = c_{u2}$	0 N*s/m	damping of the front tire
DV_cu_r	$c_{u3} = c_{u4}$	0 N*s/m	damping of the rear tire
DV_mc	m_c	8000 kg	mass of the chassis
DV_ks_f	$k_{s1} = k_{s2}$	200000 N/m	stiffness of the front suspension
DV_cs_f	$c_{s1} = c_{s2}$	20000 N*s/m	damping of the front suspension
DV_ks_r	$k_{s3} = k_{s4}$	300000 N/m	stiffness of the rear suspension
DV_cs_r	$c_{s3} = c_{s4}$	30000 N*s/m	damping of the rear suspension
DV_Icxx	$(\tilde{\tilde{I}}_c)_{xx}$	4000 kg*m2	Moment of inertia of the chassis around the x-axis (roll)
DV_Icyy	$(\tilde{\tilde{I}}_c)_{yy}$	3600 kg*m2	Moment of inertia of the chassis around the y-axis (pitch)
DV_Iczz	$(\tilde{\tilde{I}}_c)_{zz}$	1000 kg*m2	Moment of inertia of the chassis around the z-axis (yaw)
DV_me	m_e	1900 kg	mass of the engine

DV_Iexx	$\left(\tilde{\tilde{I}}_e\right)_{xx}$	151 kg*m2	Moment of inertia of the engine
DV_Ieyy	$\left(\tilde{\tilde{I}}_e\right)_{yy}$	604 kg*m2	Moment of inertia of the engine
DV_Iezz	$\left(\tilde{\tilde{I}}_e\right)_{zz}$	570 kg*m2	Moment of inertia of the engine
DV_Iexy	$\left(\tilde{\tilde{I}}_e\right)_{xy}$	0 kg*m2	Moment of inertia of the engine
DV_Iexz	$\left(\tilde{\tilde{I}}_e\right)_{xz}$	0 kg*m2	Moment of inertia of the engine
DV_Ieyz	$\left(\tilde{\tilde{I}}_e\right)_{yz}$	0 kg*m2	Moment of inertia of the engine
DV_ex	$(\tilde{e})_x$	1.809 m	x-position of the engine CM w.r.t. the CM of the chassis
DV_ey	$(\tilde{e})_y$	0 m	y-position of the engine CM w.r.t. the CM of the chassis
DV_ez	$(\tilde{e})_z - z_{c0}$	0.45 m	z-position of the engine CM w.r.t. the CM of the chassis
DV_Ke1xx	$\left(\tilde{\tilde{K}}_{e1}\right)_{xx}$	1000000 N/m	translational stiffness on the 1st mount w.r.t the global co-ordinate system
DV_Ke1yy	$\left(\tilde{\tilde{K}}_{e1}\right)_{yy}$	1000000 N/m	translational stiffness on the 1st mount w.r.t the global co-ordinate system
DV_Ke1zz	$\left(\tilde{\tilde{K}}_{e1}\right)_{zz}$	3660000 N/m	translational stiffness on the 1st mount w.r.t the global co-ordinate system
DV_Ke2xx	$\left(\tilde{\tilde{K}}_{e2}\right)_{xx}$	4290000 N/m	translational stiffness on the 2nd mount w.r.t the global co-ordinate system
DV_Ke2yy	$\left(\tilde{\tilde{K}}_{e2}\right)_{yy}$	4290000 N/m	translational stiffness on the 2nd mount w.r.t the global co-ordinate system
DV_Ke2zz	$\left(\tilde{\tilde{K}}_{e3}\right)_{zz}$	2210000 N/m	translational stiffness on the 2nd mount w.r.t the global co-ordinate system
DV_Ke3xx	$\left(\tilde{\tilde{K}}_{e3}\right)_{xx}$	4290000 N/m	translational stiffness on the 3ed mount w.r.t the global co-ordinate system

DV_Ke3yy	$\left(\tilde{\tilde{K}}_{e3}\right)_{yy}$	4290000 N/m	translational stiffness on the 3ed mount w.r.t the global co-ordinate system
DV_Ke3zz	$\left(\tilde{\tilde{K}}_{e3}\right)_{zz}$	2210000 N/m	translational stiffness on the 3ed mount w.r.t the global co-ordinate system
DV_Ce1xx	$\left(\tilde{\tilde{C}}_{e1}\right)_{xx}$	1670 N*s/m	translational damping on the 1st mount w.r.t the global co-ordinate system
DV_Ce1yy	$\left(\tilde{\tilde{C}}_{e1}\right)_{yy}$	1670 N*s/m	translational damping on the 1st mount w.r.t the global co-ordinate system
DV_Ce1zz	$\left(\tilde{\tilde{C}}_{e1}\right)_{zz}$	6120 N*s/m	translational damping on the 1st mount w.r.t the global co-ordinate system
DV_Ce2xx	$\left(\tilde{\tilde{C}}_{e2}\right)_{xx}$	5370 N*s/m	translational damping on the 2nd mount w.r.t the global co-ordinate system
DV_Ce2yy	$\left(\tilde{\tilde{C}}_{e2}\right)_{yy}$	5370 N*s/m	translational damping on the 2nd mount w.r.t the global co-ordinate system
DV_Ce2zz	$\left(\tilde{\tilde{C}}_{e2}\right)_{zz}$	2770 N*s/m	translational damping on the 2nd mount w.r.t the global co-ordinate system
DV_Ce3xx	$\left(\tilde{\tilde{C}}_{e3}\right)_{xx}$	5370 N*s/m	translational damping on the 3ed mount w.r.t the global co-ordinate system
DV_Ce3yy	$\left(\tilde{\tilde{C}}_{e3}\right)_{yy}$	5370 N*s/m	translational damping on the 3ed mount w.r.t the global co-ordinate system
DV_Ce3zz	$\left(\tilde{\tilde{C}}_{e3}\right)_{zz}$	2770 N*s/m	translational damping on the 3ed mount w.r.t the global co-ordinate system
DV_rc1x	$(\tilde{r}_{c1})_x$	2.749 m	x-position of mount 1 w.r.t. the cm of the chassis
DV_rc1y	$(\tilde{r}_{c1})_y$	0 m	y-position of mount 1 w.r.t. the cm of the chassis
DV_rc1z	$(\tilde{r}_{c1})_z$	0.075 m	z-position of mount 1 w.r.t. the cm of the chassis

DV_rc2x	$(\tilde{r}_{c2})_x$	1.549 m	x-position of mount 2 w.r.t. the cm of the chassis
DV_rc2y	$(\tilde{r}_{c2})_y$	0.25 m	y-position of mount 2 w.r.t. the cm of the chassis
DV_rc2z	$(\tilde{r}_{c2})_z$	0.375 m	z-position of mount 2 w.r.t. the cm of the chassis
DV_rc3x	$(\tilde{r}_{c3})_x$	1.549 m	x-position of mount 3 w.r.t. the cm of the chassis
DV_rc3y	$(\tilde{r}_{c3})_y$	-0.25 m	y-position of mount 3 w.r.t. the cm of the chassis
DV_rc3z	$(\tilde{r}_{c3})_z$	0.375 m	z-position of mount 3 w.r.t. the cm of the chassis

8.4 Preload of the suspensions and tires

Preloads are needed at the suspension and tires to get the position of chassis at the static equilibrium as wanted. Since the suspension and tires are spring in series, their forces are equal except the weight force of the unsprung mass. The preloads of the tires are about $m_{ui} * g$ bigger as those of the suspension.

Actually the chassis is statically indeterminate, since three equations, describing the forces as they are shown in Figure 37, can be found but there are four unknowns (Fs1, Fs2, Fs3, Fs4). That means one assumption has to be made to get a unique solution for the preloads.

This assumption is that the distribution of the static load between right and the left wheel is the same on the front and rear axle.

That can be expressed as follows:

$$\frac{F_{s1}}{F_{s2}} = \frac{F_{s4}}{F_{s3}}$$

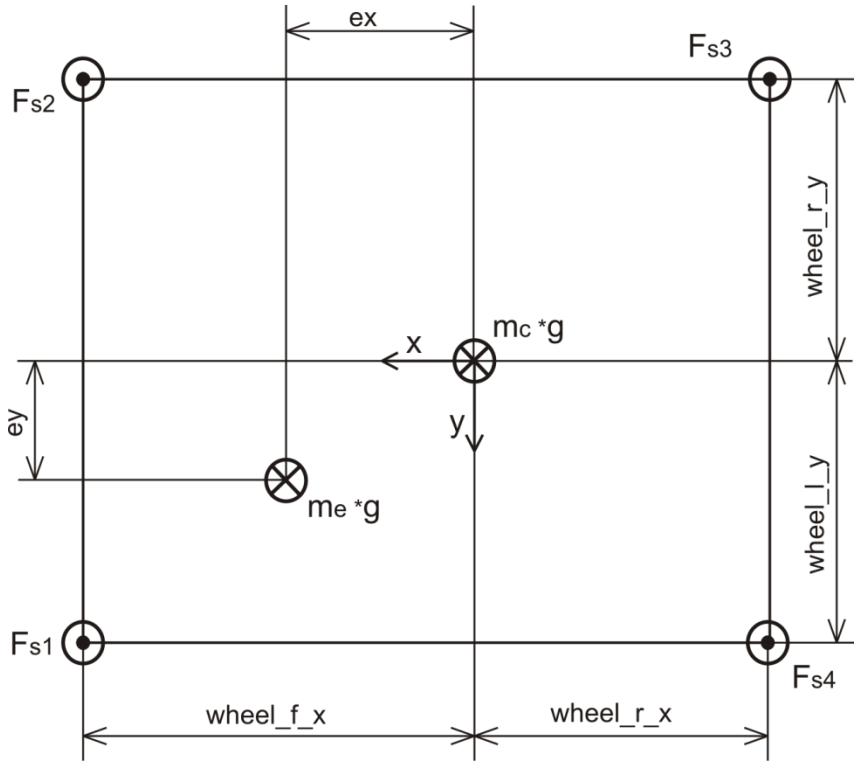

Figure 37: Preload of the suspension

The equilibriums of forces and torques give the following equations:

$$\sum F_z = 0 \quad \Rightarrow m_c g + m_e g = F_{s1} + F_{s2} + F_{s3} + F_{s4}$$

$$\sum M_x = 0 \; = (F_{s1} + F_{s4})\text{wheel\_l\_y} + (F_{s2} + F_{s3})\text{wheel\_r\_y} - m_e g\, ey$$

$$\sum M_y = 0 \; = \; (F_{s1} + F_{s2})\text{wheel\_f\_x} + (F_{s3} + F_{s4})\text{wheel\_r\_x} - m_e g\, ex$$

Those four equations result in the following preloads in z direction:

$$F_{s1} = g\frac{m_c{}^2\, rx\, ry + m_e{}^2(rx\, ry - rx\, ey - ry\, ex + ex\, ey) + m_c\, m_e(-rx\, ey + 2\, rx\, ry - ry\, ex)}{(fx - rx)(ly - ry)(m_c + m_e)}$$

$$F_{s2} = -g\frac{m_c{}^2\, rx\, ly + m_e{}^2(rx\, ly - rx\, ey - ly\, ex + ex\, ey) + m_c\, m_e(-rx\, ey + 2\, rx\, ly - ly\, ex)}{(fx - rx)(ly - ry)(m_c + m_e)}$$

$$F_{s3} = g\frac{m_c{}^2\, fx\, ly + m_e{}^2(fx\, ly - fx\, ey - ly\, ex + ex\, ey) + m_c\, m_e(-fx\, ey + 2\, fx\, ly - ly\, ex)}{(fx - rx)(ly - ry)(m_c + m_e)}$$

$$F_{s4} = -g\frac{m_c{}^2\, fx\, ry + m_e{}^2(fx\, ry - fx\, ey - ry\, ex + ex\, ey) + m_c\, m_e(-fx\, ey + 2\, fx\, ry - ry\, ex)}{(fx - rx)(ly - ry)(m_c + m_e)}$$

With the abbreviations:

wheel_f_x → fx

wheel_r_x → rx

wheel_l_y → ly

wheel_r_y → ry

8.4.1 The suspension preloads in Adams

Front left:

(9.80665 * ((DV_mc**2 * DV_wheel_r_x * DV_wheel_r_y + DV_me**2 * (DV_wheel_r_x * DV_wheel_r_y - DV_wheel_r_x * DV_ey - DV_wheel_r_y * DV_ex + DV_ex * DV_ey) + DV_mc * DV_me * (-DV_wheel_r_x * DV_ey + 2 * DV_wheel_r_x * DV_wheel_r_y - DV_wheel_r_y * DV_ex)) / ((DV_wheel_f_x - DV_wheel_r_x) * (DV_wheel_l_y - DV_wheel_r_y) * (DV_me + DV_mc))))

Front right:

(-9.80665 * ((DV_mc**2 * DV_wheel_r_x * DV_wheel_l_y + DV_me**2 * (DV_wheel_r_x * DV_wheel_l_y - DV_wheel_r_x * DV_ey - DV_wheel_l_y * DV_ex + DV_ex * DV_ey) + DV_mc * DV_me * (-DV_wheel_r_x * DV_ey + 2 * DV_wheel_r_x * DV_wheel_l_y - DV_wheel_l_y * DV_ex)) / ((DV_wheel_f_x - DV_wheel_r_x) * (DV_wheel_l_y - DV_wheel_r_y) * (DV_me + DV_mc))))

Rear right:

(9.80665 * ((DV_mc**2 * DV_wheel_f_x * DV_wheel_l_y + DV_me**2 * (DV_wheel_f_x * DV_wheel_l_y - DV_wheel_f_x * DV_ey - DV_wheel_l_y * DV_ex + DV_ex * DV_ey) + DV_mc * DV_me * (-DV_wheel_f_x * DV_ey + 2 * DV_wheel_f_x * DV_wheel_l_y - DV_wheel_l_y * DV_ex)) / ((DV_wheel_f_x - DV_wheel_r_x) * (DV_wheel_l_y - DV_wheel_r_y) * (DV_me + DV_mc))))

Rear left:

(-9.80665 * ((DV_mc**2 * DV_wheel_f_x * DV_wheel_r_y + DV_me**2 * (DV_wheel_f_x * DV_wheel_r_y - DV_wheel_f_x * DV_ey - DV_wheel_r_y * DV_ex + DV_ex * DV_ey) + DV_mc * DV_me * (-DV_wheel_f_x * DV_ey + 2 * DV_wheel_f_x * DV_wheel_r_y - DV_wheel_r_y * DV_ex)) / ((DV_wheel_f_x - DV_wheel_r_x) * (DV_wheel_l_y - DV_wheel_r_y) * (DV_me + DV_mc))))

8.4.2 The tire preloads in Adams

Front left:

(9.80665 * ((DV_mc**2 * DV_wheel_r_x * DV_wheel_r_y + DV_me**2 * (DV_wheel_r_x * DV_wheel_r_y - DV_wheel_r_x * DV_ey - DV_wheel_r_y * DV_ex + DV_ex * DV_ey) + DV_mc * DV_me * (-DV_wheel_r_x * DV_ey + 2 * DV_wheel_r_x * DV_wheel_r_y - DV_wheel_r_y * DV_ex)) / ((DV_wheel_f_x - DV_wheel_r_x) * (DV_wheel_l_y - DV_wheel_r_y) * (DV_me + DV_mc))) +9.80665*DV_m_us_f)

Front right:

(-9.80665 * ((DV_mc**2 * DV_wheel_r_x * DV_wheel_l_y + DV_me**2 * (DV_wheel_r_x * DV_wheel_l_y - DV_wheel_r_x * DV_ey - DV_wheel_l_y * DV_ex + DV_ex * DV_ey) + DV_mc * DV_me * (-DV_wheel_r_x * DV_ey + 2 * DV_wheel_r_x * DV_wheel_l_y - DV_wheel_l_y *

DV_ex)) / ((DV_wheel_f_x - DV_wheel_r_x) * (DV_wheel_l_y - DV_wheel_r_y) * (DV_me + DV_mc))) +9.80665*DV_m_us_f)

Rear right:

(9.80665 * ((DV_mc**2 * DV_wheel_f_x * DV_wheel_l_y + DV_me**2 * (DV_wheel_f_x * DV_wheel_l_y - DV_wheel_f_x * DV_ey - DV_wheel_l_y * DV_ex + DV_ex * DV_ey) + DV_mc * DV_me * (-DV_wheel_f_x * DV_ey + 2 * DV_wheel_f_x * DV_wheel_l_y - DV_wheel_l_y * DV_ex)) / ((DV_wheel_f_x - DV_wheel_r_x) * (DV_wheel_l_y - DV_wheel_r_y) * (DV_me + DV_mc))) +9.80665*DV_m_us_r)

Rear left:

(-9.80665 * ((DV_mc**2 * DV_wheel_f_x * DV_wheel_r_y + DV_me**2 * (DV_wheel_f_x * DV_wheel_r_y - DV_wheel_f_x * DV_ey - DV_wheel_r_y * DV_ex + DV_ex * DV_ey) + DV_mc * DV_me * (-DV_wheel_f_x * DV_ey + 2 * DV_wheel_f_x * DV_wheel_r_y - DV_wheel_r_y * DV_ex)) / ((DV_wheel_f_x - DV_wheel_r_x) * (DV_wheel_l_y - DV_wheel_r_y) * (DV_me + DV_mc))) +9.80665*DV_m_us_r)

8.5 Preload of the engine mounts

Preloads are needed at the mounts to get the position of engine at the static equilibrium as wanted.

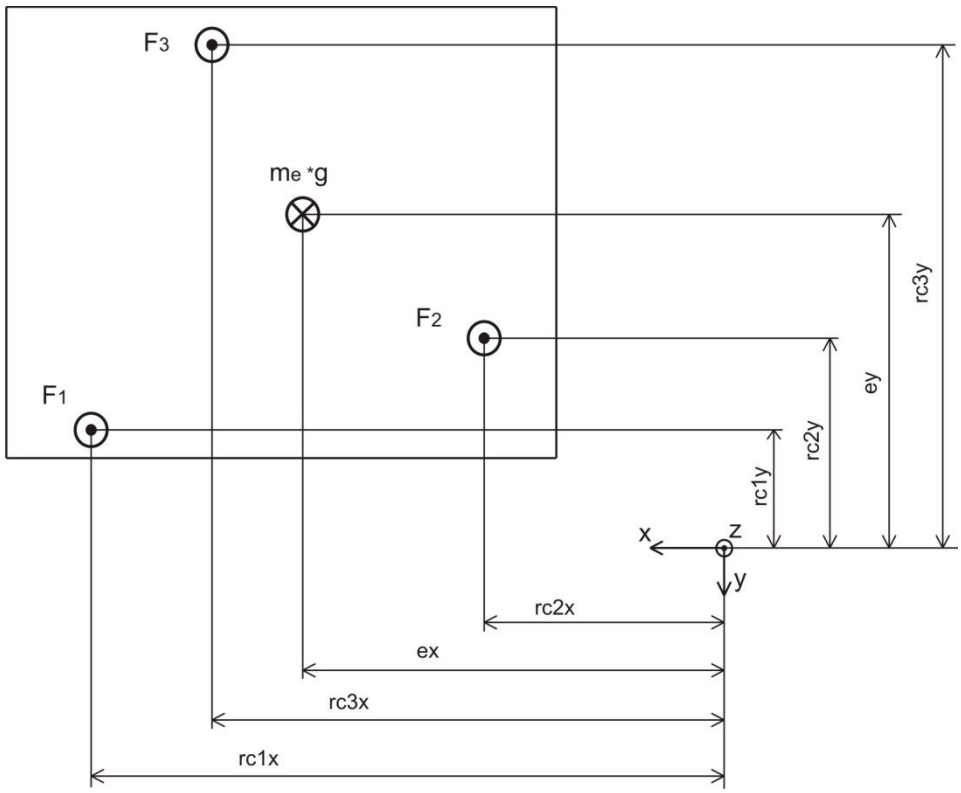

Figure 38: Preload of the engine mounts

$$\sum F_z = 0 \quad \Rightarrow m_e g = F_1 + F_2 + F_3$$

$$\sum M_x = 0 = F_1(rc1y - ey) + F_2(rc2y - ey) + F_3(rc3y - ey)$$

$$\sum M_y = 0 = F_1(rc1x - ex) + F_2(rc2x - ex) + F_3(rc3x - ex)$$

That results in the preloads in z direction:

$$F_1 = \frac{m_e g(-rc2y * rc3x + rc2x * rc3y - rc3y * ex + ey * rc3x + rc2y * ex - rc2x * ey)}{rc2y * rc1x - rc2y * rc3x + rc1y * rc3x - rc1x * rc3y + rc2x * rc3y - rc2x * rc1y}$$

$$F_2 = \frac{-m_e g(rc1y * ex - rc1y * rc3x - rc1x * ey - rc3y * ex + ey * rc3x + rc1x * rc3y)}{rc2y * rc1x - rc2y * rc3x + rc1y * rc3x - rc1x * rc3y + rc2x * rc3y - rc2x * rc1y}$$

$$F_3 = \frac{m_e g(rc2y * rc1x - rc2y * ex - rc1x * ey + rc1y * ex + rc2x * ey - rc2x * rc1y)}{rc2y * rc1x - rc2y * rc3x + rc1y * rc3x - rc1x * rc3y + rc2x * rc3y - rc2x * rc1y}$$

8.6 Total forces of the engine mounts in Adams

F1x =

-DV_Ke1xx*DX(PART_engine.MARKER_re1, PART_chassis.MARKER_rc1, PART_chassis.MARKER_rc1) -DV_Ce1xx*VX(PART_engine.MARKER_re1, PART_chassis.MARKER_rc1, PART_chassis.MARKER_rc1, PART_chassis.MARKER_rc1)

F1y =

-DV_Ke1yy*DY(PART_engine.MARKER_re1, PART_chassis.MARKER_rc1, PART_chassis.MARKER_rc1) -DV_Ce1yy*VY(PART_engine.MARKER_re1, PART_chassis.MARKER_rc1, PART_chassis.MARKER_rc1, PART_chassis.MARKER_rc1)

F1z =

-DV_Ke1zz*DZ(PART_engine.MARKER_re1, PART_chassis.MARKER_rc1, PART_chassis.MARKER_rc1) -DV_Ce1zz*VZ(PART_engine.MARKER_re1, PART_chassis.MARKER_rc1, PART_chassis.MARKER_rc1, PART_chassis.MARKER_rc1) +(DV_me*9.80665*(-DV_rc2y*DV_rc3x +DV_rc2x*DV_rc3y -DV_rc3y*DV_ex +DV_ey*DV_rc3x +DV_rc2y*DV_ex -DV_rc2x*DV_ey) /(DV_rc2y*DV_rc1x -DV_rc2y*DV_rc3x +DV_rc1y*DV_rc3x -DV_rc1x*DV_rc3y +DV_rc2x*DV_rc3y -DV_rc2x*DV_rc1y))

F2x =

-DV_Ke2xx*DX(PART_engine.MARKER_re2, PART_chassis.MARKER_rc2, PART_chassis.MARKER_rc2) -DV_Ce2xx*VX(PART_engine.MARKER_re2, PART_chassis.MARKER_rc2, PART_chassis.MARKER_rc2, PART_chassis.MARKER_rc2)

F2y =

-DV_Ke2yy*DY(PART_engine.MARKER_re2, PART_chassis.MARKER_rc2, PART_chassis.MARKER_rc2) -DV_Ce2yy*VY(PART_engine.MARKER_re2, PART_chassis.MARKER_rc2, PART_chassis.MARKER_rc2, PART_chassis.MARKER_rc2)

F2z =

-DV_Ke2zz*DZ(PART_engine.MARKER_re2, PART_chassis.MARKER_rc2, PART_chassis.MARKER_rc2) -DV_Ce2zz*VZ(PART_engine.MARKER_re2, PART_chassis.MARKER_rc2, PART_chassis.MARKER_rc2, PART_chassis.MARKER_rc2) +(-DV_me*9.80665*(DV_rc1y*DV_ex -DV_rc1y*DV_rc3x -DV_rc1x*DV_ey -DV_rc3y*DV_ex +DV_ey*DV_rc3x +DV_rc1x*DV_rc3y) /(DV_rc2y*DV_rc1x -DV_rc2y*DV_rc3x +DV_rc1y*DV_rc3x -DV_rc1x*DV_rc3y +DV_rc2x*DV_rc3y -DV_rc2x*DV_rc1y))

F3x =

-DV_Ke3xx*DX(PART_engine.MARKER_re3, PART_chassis.MARKER_rc3, PART_chassis.MARKER_rc3) -DV_Ce3xx*VX(PART_engine.MARKER_re3, PART_chassis.MARKER_rc3, PART_chassis.MARKER_rc3, PART_chassis.MARKER_rc3)

F3y =

-DV_Ke3yy*DY(PART_engine.MARKER_re3, PART_chassis.MARKER_rc3, PART_chassis.MARKER_rc3) -DV_Ce3yy*VY(PART_engine.MARKER_re3, PART_chassis.MARKER_rc3, PART_chassis.MARKER_rc3, PART_chassis.MARKER_rc3)

F3z =

-DV_Ke3zz*DZ(PART_engine.MARKER_re3, PART_chassis.MARKER_rc3, PART_chassis.MARKER_rc3) -DV_Ce3zz*VZ(PART_engine.MARKER_re3, PART_chassis.MARKER_rc3, PART_chassis.MARKER_rc3, PART_chassis.MARKER_rc3) +(DV_me*9.80665*(DV_rc2y*DV_rc1x -DV_rc2y*DV_ex -DV_rc1x*DV_ey +DV_rc1y*DV_ex +DV_rc2x*DV_ey -DV_rc2x*DV_rc1y) /(DV_rc2y*DV_rc1x -DV_rc2y*DV_rc3x +DV_rc1y*DV_rc3x -DV_rc1x*DV_rc3y +DV_rc2x*DV_rc3y -DV_rc2x*DV_rc1y))